Journal of Cardiovascular Magnetic Resonance®, 4(3), 381–410 (2002)

REVIEW ARTICLE

The Assessment of Myocardial Viability: A Review of Current Diagnostic Imaging Approaches

Rebecca E. Thornhill,[1,2,*] Frank S. Prato,[1,3] and Gerald Wisenberg[1,2,3]

[1]*Department of Nuclear Medicine and Magnetic Resonance, Imaging Division, Lawson Health Research Institute, St. Joseph's Health Care, London, Ontario, Canada*
[2]*Department of Medical Biophysics, University of Western Ontario, London, Ontario, Canada*
[3]*Division of Cardiology, London Health Sciences Centre, University Campus, London, Ontario, Canada*

ABSTRACT

The management of patients with coronary artery disease, both in the post-infarction setting, and in patients with chronic advanced left ventricular (LV) dysfunction, is complicated by the presence of both reversibly damaged and infarcted myocardium. Although acute revascularization with thrombolytic therapy and percutaneous angioplasty have served to reduce the overall mortality from myocardial infarction, the ability to predict whether or not dysfunctional myocardium will recover following revascularization presents the clinician with a serious challenge. The success of revascularization, both on improvement of LV function, and short and long-term prognosis, depends on both the existence and extent of viable but dysfunctional myocardium present, as there is little to be gained from revascularizing a territory consisting exclusively of scar. There is a clear demand for procedures that can identify reversible asynergy prospectively and thus deliver the information that is needed for clinical decision-making. The objective of this review is to summarize the diagnostic tools that are currently available for the identification of reversible injury (i.e., stunned or hibernating myocardium). The relative merits of echocardiography, nuclear medicine imaging, and magnetic

*Corresponding author. Department of Nuclear Medicine and Magnetic Resonance, St. Joseph's Health Care London, 268 Grosvenor St., London, Ontario, Canada, N6A 4V2. Fax: +1-519-646-6135; E-mail: rthornhi@lri.sjhc.london.on.ca

resonance imaging are discussed in detail. Within the discussion of each modality, special attention is paid to the more recent innovations that have arisen to enhance the diagnostic and prognostic value of older approaches. Cost, availability, and local expertise will always affect the clinical popularity of a given diagnostic approach. However, the overriding conclusion that emerges from this review is that the future "techniques of choice" will be those that can reliably predict and quantify the extent of potential functional recovery.

Key Words: *Myocardial viability; Cardiac imaging; Coronary artery disease; Stunned myocardium; Hibernating myocardium*

OVERVIEW

The ability to distinguish reversible from irreversible myocardial injury is of critical importance in the management of patients with both acute and chronic coronary artery disease (CAD) syndromes. The most important variable influencing long-term outcomes in patients with coronary disease is the status of left ventricular (LV) function. Impairment of LV function is clearly associated with a reduction in both quality and quantity of life. Interventions that improve LV function have consistently shown benefits on hard patient outcomes, i.e., survival, and softer outcomes, such as admission rates for congestive heart failure, and quality of life indicators, including heart failure classifications, and exercise capacity.[1–10] As well, there may very well be alternative or supplemental means of improving LV function and prognosis that may follow from our improved understanding of the complex interrelationships between myocardial perfusion, metabolism, cell membrane and vascular integrity, and systolic function.

The goal of this review is to provide a survey of the techniques that are currently available for the clinical assessment of myocardial viability. Before we address the relative merits of these techniques, it is first important to appreciate the pathophysiology that these tools are designed to interrogate. To this end, we begin with a brief discussion regarding the evolution of myocardial injury—from the onset of ischemia to reversible damage and, finally, necrosis.

THE MYOCARDIAL RESPONSE TO ISCHEMIC INJURY

Reversible Injury

Within seconds of the onset of severe ischemia, there is an abrupt change from predominantly aerobic to anaerobic metabolism. This results in a drastic decrease in the production of high-energy phosphates (HEP), namely adenosine triphosphate (ATP) and phosphocreatine (PCr).[11] Reversible injury is difficult to identify with light microscopy, although disturbances in fluid and ionic homeostasis may manifest in water vacuoles (hydropic change) and cellular swelling. Electron microscopy is best suited to identify the ultrastructural changes associated with reversible injury, namely mitochondrial swelling, loosening of intercellular attachments, the presence of small, lipid-rich amorphous mitochondrial densities, dilation of the sarcoplasmic reticulum (SR), disaggregation of SR polysomes, and myofibrillar relaxation.[11,12] In canine models of severe ischemia [i.e., flow ($\leq 10\%$ normal)], these ultrastructural defects are entirely reversible if reperfusion occurs within 20–40 min. The myocardium is functionally sensitive to ischemia, however, and will exhibit marked contractile dysfunction within 1 min of acute onset.[11] The length of time this contractile impairment remains is profoundly influenced by the severity and duration of the ischemic period and clearly, by the development of irreversible injury.

Irreversible Injury

Irreversible injury, i.e., infarction, follows a distinct geographic pattern in the myocardium, beginning in subendocardial tissue and progressing towards the subepicardium. In canine, experimental models of acute myocardial infarction (AMI), myofibril death begins after approximately 40 min and reaches its full, transmural extent in as little as 3–6 hr. The time-course is somewhat more protracted in humans, taking generally as long as 6–12 hr for complete infarction of the myocardium at risk.[13] Despite the presence of markers of loss of cellular integrity, i.e., cardiac enzymes and proteins in the serum as early as 2 hr post-infarction, the necrotic changes are seldom evident, histologically, until at least 4–12 hr after onset.[14]

The microscopic changes associated with irreversible myocyte damage include the denaturation of cytoplasmic proteins, swelling, and enzymatic digestion of organelles and the sarcolemma. On a gross level, immature myocardial infarcts have poorly defined borders. The margins of the infarct demonstrate inflammatory hyperemia, which is incited by the necrotic tissue itself. With time, macrophages will arrive on the scene of injury and engulf the remaining cellular debris.[11,14] Finally, connective tissue grows into the area of fibrinous exudate, ultimately transforming the original site of necrosis into a mature, collagenous, noncontractile scar.

In addition to the obvious early necrotic process, apoptosis or "programmed cell death," is now recognized as a consequence of ischemia and reperfusion. Unlike necrosis, however, the apoptotic process incites no inflammatory reaction and it is therefore much more difficult to identify with conventional histology. Techniques that detect DNA fragmentation—a hallmark of apoptosis—have confirmed that it is a contributor to irreversible injury in the setting of AMI.[15] The time course of the apoptotic cascade in the context of myocardial ischemia is still largely unclear. In the greater scheme of irreversible ischemic damage, apoptosis is believed to contribute very little, on the order of $\sim 8\%$ of total myocyte deaths.[16] However, a large number of earlier basic studies of myocardial infarction using isolated heart preparations or intact animal models may have underestimated the extent of myocardial necrosis by not waiting a sufficiently long period of time for the evolution of apoptosis, a process that appears to require at least days to become manifest.

Reperfusion

The overwhelming priority in the acute management of patients post-AMI is to limit the extent of necrosis. With severe ischemia of less than approximately 6 hr duration, restoring the blood supply to normal- or near normal-levels can salvage at least some fraction of the area at risk.[11,17,18] Thrombolytic therapy or angioplasty are frequently used when electrocardiographic evidence of transmural ischemia is evident, in an attempt to establish reperfusion.

MYOCARDIAL VIABILITY

Central to the issue of undertaking interventional procedures after an AMI, or in the presence of chronic ischemia-mediated LV dysfunction is the question of *viability*. If tissue is viable, it will benefit through improvement in function by restoration of normal blood flow. Indirectly, in theory, the patient's prognosis will also improve, with an increase in ejection fraction, systolic and diastolic performance, exercise capacity, and most importantly, survival.

It is generally agreed that, in order for myocardium to be considered viable, it must: (1) have the ability to generate HEP (i.e., PCr and ATP), (2) have an intact sarcolemma, in order to maintain ionic/electrochemical gradients, and (3) have sufficient perfusion, both for the delivery of substrates and O_2 and for the adequate washout of potentially noxious metabolites.[17,19] An obvious omission from this list of criteria is the issue of contractility. There are two tissue states that exhibit sustained contractile dysfunction despite meeting the three criteria listed above: stunned and hibernating myocardium. Myocardial stunning was a phenomenon first documented by Heyndrickx et al. in the mid-1970s[20] but was not given this label until 1982, when Braunwald and Kloner defined stunned myocardium as tissue which exhibits prolonged contractile dysfunction after a transient ischemic insult and coronary reperfusion.[21] That is, despite a prompt and complete return of blood flow, it can take days and even weeks for the injured myocardium to recover its native contractile abilities.

By contrast, the second type of reversibly damaged myocardium, "hibernating" myocardium, has been typically characterized as secondary to reduced coronary perfusion. Hibernating myocardium exhibits persistent dysfunction at rest and at stress but this can be either partially or completely restored by revascularization interventions (e.g., angioplasty or coronary artery bypass graft, CABG).[22,23] Some have also proposed that hibernation develops following recurrent intermittent episodes of profound ischemia and is, in essence, a consequence of repetitive periods of stunning.[24]

It is clear from the foregoing discussion that for the ideal evaluation of viability, one would wish to have a complete set of data regarding perfusion, metabolic status, and cellular membrane integrity. Much of this review will focus on the techniques available to provide us with this data.

Myocardial Stunning

Although the stunning phenomenon was first documented in experimental canine models of short-term ischemia and reperfusion, post-ischemic contractile dysfunction has been observed in many different clinical

situations, especially in the following examples: 1) unstable angina,[25] 2) exercise-induced ischemia,[26] 3) cardiac surgery patients, if a cardioplegic solution has been used,[27] and 4) reperfused-AMI.[28] In the first two cases, regional LV dysfunction can be induced by transient ischemia but systolic and diastolic dysfunction can persist for hours after chest pain and electrocardiograph (ECG) changes have resolved.[29] Global contractile dysfunction is not an uncommon consequence of cardiac surgery, when cardioplegic solutions are used to temporarily arrest the heart. This has led to the increasing performance of surgery on the beating heart, to lessen the detrimental effects on post-operative contractile function, even if they are transient. Regional ventricular stunning is often observed when AMI patients receive thrombolytic or angioplasty treatment. In the early period post-reperfusion, the contractile dysfunction caused by stunning can be difficult to impossible to differentiate from that which is due to infarction.

The time-course of myocardial stunning in humans is thought to be more unpredictable than that observed in animal models: dysfunction may persist for hours or for as long as 6 weeks post-insult.[30] In general, both the duration and severity of ischemia determine the duration of post-ischemia/reperfusion dysfunction.[31] Interestingly, there is recent evidence to suggest that stunning may contribute to the dysfunction observed in cases of heart failure, particularly ischemic cardiomyopathy.[32] The difficulty in assessing *simultaneously* perfusion and function has limited the recognition of stunning in clinical contexts.

Several hypotheses have emerged to explain the contractile dysfunction that follows short-term ischemia and reperfusion. Early work focused on the metabolic derangement that is correlated with stunning.[11,33–39] Much more recent work has identified the deleterious effects of oxyradical production on the contractile elements of the myocardium.[40–45] In tandem, and not in contradiction, the latest research is strengthening the hypothesis that myofilament sensitivity to Ca^{2+} is abnormal in stunned myocardium.[46,47] For more discussion regarding the candidate mechanisms for stunning, the reader is directed to a thorough review by Bolli and Marban.[47]

Hibernating Myocardium

As originally defined by Rahimtoola,[23] hibernating tissue exhibits marked contractile dysfunction as a result of chronic hypoperfusion that will improve or normalize after revascularization. It is believed to represent an adapted state, one in which contractile function is diminished in order to "match" the decreased supply of substrates and O_2 to the myocardium. In addition to down-regulating contraction, Casey and Arthur[48] have shown that hibernating myocytes exhibit diminished protein and mRNA synthesis.

Hibernation is thought to be distinct from myocardial stunning, where the decrease in supply is severe and transient. Recent evidence suggests alternate explanations for this phenomenon. One proposal contends that resting myocardial perfusion may actually be normal and that it is perfusion *reserve* that is inadequate in this tissue state[49,50] leading to ischemia when tissue demand increases. The other postulate is that hibernation has occurred secondary to recurrent severe ischemia in the setting of a severe coronary stenosis, exposed to intermittent total or sub-total occlusion because of transient thrombus.[24]

The cytological changes characteristic of hibernating myocardium are profound but reversible in nature. It has been shown that there is a progressive loss of contractile proteins that occurs, oddly, without a marked decrease in cell volume. Rather, the space previously occupied by the sarcomeres is predominantly replaced by glycogen. There are also changes in the extracellular matrix of hibernating myocardium, with an increase in the amount of both collagen and proteoglycans.[51] Eventually, the cardiac myocytes that comprise hibernating myocardium resemble those of fetal hearts: they begin to "de-differentiate."[52] This is significant because the time-course of recovery following revascularization may depend on the time required to resynthesize and express new contractile material. Although the time to recovery of function may be nearly immediate for a subset of patients, post-revascularization, others follow a much more protracted (up to 10 weeks) course of recovery.[53] Histopathologic studies have identified discrete stages of degeneration within the framework of hibernation itself, with each progressive stage characterized by less contractile protein and more fibronectin and collagen I.[54]

IDENTIFYING VIABLE MYOCARDIUM

Fully understanding the mechanisms leading to myocardial stunning and hibernation is not merely an academic exercise; in 1998, the National Heart, Lung and Blood Institute held a workshop in order to discuss current thinking about reversible myocardial injury. The following was among their recommendations for future

research: "To develop better methods for the diagnosis of stunning in humans, including the development of diagnostic techniques that can rapidly distinguish stunning from necrosis after cardiac surgery and after revascularization for AMI. In these situations, such a distinction is essential for selecting the proper management of patients with severe LV dysfunction or cardiogenic shock. Better diagnostic methods that can distinguish stunning from hibernation would also help to define the prevalence, natural history, and clinical importance of these two conditions; ideally, these diagnostic methods should be accurate, relatively inexpensive, and broadly available."[32]

Further, the enhanced understanding of the complex interrelationships between myocardial perfusion, cell membrane and metabolic integrity, and systolic and diastolic function will hopefully lead to metabolic interventions which will lead to improvements in myocardial function and patient prognosis.

THE ASSESSMENT OF MYOCARDIAL VIABILITY

The assessment of myocardial viability (extent of infarction) must include an assessment of coronary artery anatomy by coronary angiography to determine the potential for revascularization in a given patient, if viability in ischemic tissue is suggested by noninvasive imaging modalities. Atherosclerosis tends to be a very diffuse process, often extending to some extent throughout the entire length of a given coronary artery, and may limit the possibility of undertaking percutaneous angioplasty or even bypass surgery.

Noninvasive techniques can only identify tissue that *might* benefit from revascularization. The gold standard for the assessment of viability, in the clinical setting, is therefore limited. The measured outcome for noninvasive testing has generally been the improvement in regional function as monitored by yet another noninvasive modality. Clinically, it is not possible to have histological verification of tissue viability. The determination of viability is indirect and depends on a given region's functional response to revascularization. This remains a limitation of all clinical studies of viability using noninvasive markers. Further, if we define the assessment of viability as the detection and discrimination of four tissue states (normal, stunned, hibernating, and infracted), then viability assessments should inherently include measurements of tissue blood flow.

Echocardiography

Echocardiography has been extremely useful in the assessment of global and regional cardiac dysfunction—an invaluable tool used to document the early and late functional changes at rest, in the absence of inotropic stimulation, which occur following AMI. Stress echocardiography with dobutamine has also been used to identify viable, yet chronically dysfunctional myocardium. By administering multiple, step-wise doses of dobutamine, hibernating tissue, dysfunctional at rest, and manifesting hypokinesis, akinesis, or even dyskinesis, may exhibit a biphasic response, responding with an improvement in contractile performance at lower doses ($5-10\ \mu$g/kg/min), only to regress when the metabolic demand stimulated at higher doses ($\geq 15\ \mu$g/kg/min) overwhelms the tissue's capacity to respond.[55] Transmural myocardial biopsies obtained from patients with hibernating myocardium have shown that tissue with $>17\%$ fibrosis failed to exhibit contractile reserve when challenged with low-dose dobutamine.[56] The importance of disease severity was further highlighted by a 1998 study of patients with post-ischemic heart failure (patients were studied pre- and 6 months post-CABG).[57] In this study, Pagano and colleagues reported that the diagnostic accuracy of dobutamine-echocardiography was reduced with increasing severity of regional and global LV dysfunction. That is, the technique appeared to underestimate the extent of viability: 39% of all recovering LV segments failed to exhibit inotropic contractile reserve. In a similar but separate study of functional recovery pre- and 6 months post-revascularization, low-dose dobutamine failed to identify 45% of the segments that ultimately regained function.[58] Thus, dobutamine-echocardiography is an easily accessible tool with sub-optimal sensitivity for the detection of residual tissue viability. Reductions in blood flow that lead to hibernation likely do so across a significant range of flows, with a corresponding spectrum of metabolic reserve. Those regions with greater metabolic reserve will likely retain the ability to respond to an inotropic stimulus while those regions with profoundly reduced flow—just on the threshold of viability—will have no ability to respond. Such regions will therefore appear to be nonviable on a dobutamine-echocardiography challenge.

There are many limitations to conventional 2D echocardiography and these may diminish its diagnostic value in the assessment of myocardial viability. The results of echocardiography are largely qualitative in nature and therefore very reliant on the interpreting

physician. Despite reports of high interobserver agreement, inter-center concordance has been evaluated at less than 80%.[59] Attempts to *quantify* contractile abnormalities include the measurement of %regional systolic wall thickening (%WT) and ejection fraction (EF%). Perhaps the greatest limitation is the necessity for a "good acoustic window," in order to evaluate LV function. Patients with a large body habitus, those with significant pulmonary disease, or those with prior cardiac surgery are poor candidates for echocardiography.[60] Approximately 15% of CAD patients are believed to have inadequate acoustic windows.[61] This can be overcome, to a great extent, by the performance of transesophageal echocardiography, which has been performed with dobutamine stimulation for the evaluation of tissue viability.[62,63]

Another major limitation of 2D echocardiography is that the endocardial/LV blood pool interface (the endocardial border) can be difficult to visualize, thus rendering quantifications of %WT and EF% less accurate. "Second-harmonic imaging," was developed in order to improve echocardiographic image quality. This technique involves the analysis of the returning acoustic signal at a frequency that is exactly double the transmitted (fundamental) frequency.[64] With increasing depth, there is more distortion of the original sound wave and, hence, more production of harmonics. Receiving the second-harmonics effectively serves to amplify the signal that is received from deeper tissue structures.[65] The improvement in endocardial border delineation is perhaps most striking in stress echocardiography examinations. Recently, Franke and colleagues performed second-harmonic imaging with dobutamine stress in a group of patients with poor transthoracic windows (determined during a traditional echo exam, in fundamental mode).[66] In this study, designed to test for the presence of coronary disease, second-harmonic imaging conferred an improvement in sensitivity over fundamental mode imaging (92 vs. 64%, respectively). The improvement in endocardial definition may enhance viability assessments with transthoracic echocardiography but this hypothesis requires validation.

Another notable advancement in echocardiography has been the development of myocardial contrast echocardiography (MCE). Briefly, microbubbles, injected intravenously, release ultrasound energy at the transmitted frequency *and* at harmonics of the transmitted frequency. Their nonlinear backscatter characteristics allow for increased contrast between tissue and the intravascular microbubbles, when used in conjunction with second-harmonic reception—the signal amplitude of the tissue at the second-harmonic frequency is much less than the signal effect caused by the contrast agent.[67]

In addition to improving the delineation of the endocardial border, microbubbles have been used to estimate myocardial perfusion and have performed well when compared to the radiolabeled microsphere standard.[68,69] Microbubble uptake has demonstrated clinical value in identifying perfusion defects after AMI: improvement in perfusion, as assessed by MCE, at least 24 hr post-AMI was predictive of subsequent functional recovery in a study of patients with first-AMI undergoing revascularization interventions.[70] In a comparison of MCE-identified perfusion defects and dobutamine-stress echocardiography, it was found that early recovery of microvascular perfusion patterns was strongly associated with myocardial viability.[71] Despite its high sensitivity, MCE has a very poor predictive value when used alone.[72,73] If applied with second-harmonic imaging, however, MCE confers impressive endocardial border delineation and can be used for *some* patients with otherwise inadequate acoustic windows.[74,75]

Single Photon Emission Computed Tomography

Single-photon emission computed tomography (SPECT), has largely replaced conventional planar scintigraphy in current clinical nuclear medicine practice. In terms of radiopharmaceuticals, the two most widely used compounds in SPECT perfusion/viability imaging of the heart are Tl-201 and Tc-99m-sestamibi.

Tl-201 Imaging

Tl-201 is the most frequently used agent in radionuclide imaging of the heart. It is a potassium analog that enters cells via the sarcolemmal Na^+/K^+ ATPase pump. As previously discussed, a disrupted sarcolemma is inconsistent with viability, and it follows that this tracer can only gain entrance into viable cells. Furthermore, the initial uptake and washout of Tl-201 (to viable myocardium) is in direct proportion to tissue blood flow, making it a suitable tracer for the study of myocardial perfusion. Due to its long half-life (73 hr), a large reservoir of Tl-201 will persist in the blood stream and following initial uptake will redistribute to the myocardium for many hours after injection.[76] Hours after the injection, myocardial Tl-201 concentrations primarily reflect viable myocardium rather than differences in tissue flow.

Imaging occurs immediately following stress, with either exercise or pharmacologically induced coronary

hyperemia with dipyridamole or adenosine, and again after 3–4 hr redistribution of Tl-201.[77] Defects that are seen on post-stress images, after ischemia has been induced, may "fill in" by the time the rest-redistribution images are acquired, indicating viability. Conversely, a defect that persists and appears again on the 3–4 hr images (i.e., a fixed-defect) reflects: (1) markedly reduced regional perfusion, (2) impaired cellular membrane integrity, inadequate for the active sequestration of the tracer into the cell, (3) cell death (acute infarction), or (4) scar tissue. Thus, fixed-defects on 3–4 hr redistribution images may represent only severely hypoperfused—and not necessarily infarcted tissue.[78]

If a fixed-defect is seen in early redistribution images, a third set of images may be acquired at 24 hr, which would allow for redistribution of the tracer to very-ischemic (yet viable) tissue.[79] It has been shown that 22% of fixed-defects (at early redistribution imaging) demonstrate normal Tl-201 uptake at later redistribution. This may indicate a poorly perfused, yet viable region.[80] Clearly, late imaging can improve the identification of viable myocardium, though even late redistribution images tend to overestimate the extent of infarction, especially in patients with subendocardial infarcts.[81]

An alternative to late redistribution imaging is to perform a second injection of Tl-201 at the 3–4 hr (early) redistribution exam,[82,83] often called a viability study. This may be necessary because redistribution depends on the continued delivery of the tracer over the 3–4 hr period. If the blood concentration of Tl-201 remains constant or increases during the period between stress and early redistribution imaging, an initial defect in a region of viable myocardium should fill-in. If the blood concentration of Tl-201 decreases a great deal, there may be insufficient delivery of the tracer and the defect may not fill-in during redistribution imaging.[82] The second injection of thallium with delayed imaging after this repeat injection will give the myocytes with reduced perfusion the greatest opportunity to sequester thallium, if they are still metabolically capable of this ATP-dependent process.

The results of Tl-201 SPECT have been very rewarding but despite the apparent demonstration of viability, many segments fail to recover in response to revascularization. This technique has a sensitivity that ranges from 64 to 72% and specificity from 45 to 88%, for improvement in contractile function.[84–87] The predictive accuracy of Tl-201 rest-redistribution imaging was found to be higher than that of low-dose dobutamine-echocardiography (77 vs. 58%), when the two techniques were compared in a population of chronic CAD patients studied before and after revascularization.[88] Pace and coworkers have previously demonstrated that higher specificity and accuracy (but lower sensitivity) can be attained by using a greater %Tl-201 uptake threshold (when classifying segments as viable or nonviable); they recommend the use of a 65% uptake threshold, rather than the 50% cutoff value that is commonly used in Tl-201 image analysis.[89]

Tc-99m-sestamibi Imaging

In contrast to Tl-201, Tc-99m-2-methoxyisobutyl isonitrile (Tc-99m-sestamibi) decays with a much shorter half-life (6 hr) and emits photons with a higher energy range (140 vs. 70 keV), providing improved imaging characteristics. Like Tl-201, the initial cellular uptake of Tc-99m-sestamibi is in direct relation to myocardial blood flow; once extracted from the blood pool, Tc-99m-sestamibi will bind to the myocyte's mitochondria, as long as the mitochondrial matrix is intact and the transmembrane potential is negatively charged,[90] so it is also a reasonable reflection of viability. Unlike Tl-201, however, Tc-99m-sestamibi becomes (very nearly) irreversibly bound, once inside the cell, so there is virtually no redistribution of this tracer.

As with Tl-201, viability imaging with Tc-99m-sestamibi can be performed at rest (only) or, more commonly, at both rest and following exercise (each obtained with separate injections). However, in a population of chronic CAD patients, Maurea and colleagues found that nitroglycerin administration improved Tc-99m-sestamibi uptake in 27% of segments with severely reduced resting uptake.[91] Furthermore, at 5 ± 3 months post-CABG, 87% of the pre-CABG, reversible defects showed significant functional recovery, thus demonstrating the impact of nitrates on the identification of dysfunctional but severely hypoperfused (hibernating) myocardium. Similar results in favor of nitrate-stress have been reported by Schneider et al.[92] and Batista et al.[93]

Some studies have demonstrated good agreement between sestamibi and Tl-201, in terms of their ability to predict future recovery following revascularization.[94,95] There is some evidence, however, that Tc-99m-sestamibi underestimates viability to a larger extent than Tl-201.[95–98] To address this concern, Udelson et al.[94] investigated the impact of %uptake threshold on the distinction between salvageable and infarcted myocardium; this group has recommended a threshold of 60%. Using this approach, Hurrell and coworkers have used Tc-99m-sestamibi to measure infarct-size in patients with chronic CAD.[99]

Tc-99m-tetrofosmin has been used in lieu of Tc-99m-sestamibi, as its kinetics are similar (uptake is related to both flow and the integrity of the sarcolemma.[100,101]) The tetrofosmin tracer was developed for its relatively fast clearance from blood and low uptake in nontarget tissue such as the liver.[102] It has been studied to a much lesser extent than Tc-99m-labeled sestamibi, particularly with regards to its role as a viability tracer, but it has proven its worth as a perfusion tracer in canine models of reperfused infarction.[103–105]

Value of Conventional SPECT Imaging

Currently, Tl-201 imaging at rest immediately after injection, and again following a 3 hr delay has evolved as the modality of choice for conventional nuclear tracer imaging.[106] The identification of viable myocardium by the Tl-201 rest/redistribution approach has been shown to predict significant improvement in functional class (New York Heart Association)[6] and in event-free survival post-CABG.[107] Furthermore, stress perfusion SPECT has proven its value in the risk-stratification of patients, particularly in predicting cardiac events, both early post-infarction[108,109] and late (>1 year) following revascularization.[110] It is notable that dobutamine-echocardiography—a less costly diagnostic test—has performed consistently worse than perfusion SPECT in predicting hard clinical outcomes.[111] It follows that, although the direct cost of radionuclide testing is higher than that of dobutamine-echocardiography, the inferior predictive value of the latter test is likely to result in greater downstream costs in the form of subsequent testing and interventions.[112]

At present, the value of either Tl-201 or Tc-99m-sestamibi in the identification of reversibly damaged myocardium is mainly limited by the spatial resolution conferred by SPECT imaging of these tracers; it is not currently possible to detect transmural variations in viability, for this reason. A small subendocardial infarct with subepicardial stunning may well appear as either normally perfused or as an area of low-count density on a SPECT image (i.e., below the 50 or 60% thresholds that are often used), but it would be unlikely to correctly delineate the limited area of infarction.

Novel Radiopharmaceuticals

Several new radiopharmaceuticals have been developed for application to cardiac SPECT assessments of viability:

(a) I-123-(*p*-iodo phenyl)-3-*R*,*S*-methylpentadecanoic acid (^{123}I-BMIPP), a fatty-acid analog: this tracer has a long retention time in tissue as it is incorporated into the triglyceride pool and partially metabolized through alpha and, later, β-oxidation into smaller catabolites. It is very sensitive to mitochondrial dysfunction. ^{123}I-BMIPP has been evaluated in canine models of mild and severe ischemia and its metabolism is closely associated with the severity of induced ischemia.[113]

(b) Tc-99m-annexin-V, an agent with a high-affinity for apoptotic cells: as discussed earlier in this review (under "Irreversible Injury"), it has become increasingly clear that apoptosis plays an important role in ischemia/reperfusion injury. Examining the extent of apoptosis post-AMI (i.e., in vivo) has not been feasible until very recently; the best one could do was to submit post-mortem myocardial samples to DNA end-labeling analysis.[114] Clinical imaging with an apoptosis-specific tracer was first attempted in a recent study of reperfused AMI patients.[115] When compared to either Tc-99m-sestamibi or tetrofosmin images, the annexin-V images demonstrated that there was no increased uptake of Tc-99m-annexin-V outside of the infarct itself.

In vitro work had previously elucidated the mechanism by which annexin-V binds specifically to apoptotic cells: annexin-V has a particularly high-affinity for cells with externalized phosphatidylserine.[116] Phosphatidylserine is normally resident on the inner-leaflet of the plasmalemma and its export to the outer-leaflet has been recognized, in vitro, as a signature of the apoptotic cell.[117] The inspiration to radiolabel annexin-V for use in clinical cardiac imaging is credited to Blankenberg et al., for their important work with Tc-99m-HYNIC-labeled annexin-V in rodent models of apoptosis.[118] While the preliminary results of Hofstra et al. are encouraging, it should be noted that annexin-V also has a high-affinity for the exposed phosphatidylserine on activated platelets—a potentially significant confound in cases of AMI, where there is most definitely platelet activation.[119]

Technical Developments with SPECT

The development of gated-SPECT has spawned a new, quantitative area of cardiac nuclear medicine. Functional assessments are now possible (e.g., %WT and EF%) and may prove immensely valuable when used in conjunction with the assessment of myocardial perfusion. Additionally, the %WT and EF% estimates obtainable by gated-SPECT are useful in patients with nondiagnostic echocardiograms (e.g., due to severe pulmonary obstructive disease or extreme obesity).[120]

By far, the greatest technical limitation of cardiac SPECT is the problem of photon attenuation, particularly in the inferior wall. Attenuation correction is becoming more available with commercial systems, although its benefits have still to be validated clinically.[79]

Positron Emission Tomography

At present, cardiac positron emission tomography (PET) imaging with the tracer ^{18}F-2-deoxy-2-fluoro-D-glucose (FDG) is considered as the gold-standard noninvasive test for the determination of myocardial viability. Although PET imaging of this type can provide extremely valuable information about viability, its use has been limited. This is largely due to the high capital and operating costs involved with this modality. Since PET imaging requires the injection of generally positron-emitting, cyclotron-produced radiopharmaceuticals, with relatively short half-lives (ranging from 2 to 110 min), the institution must have a cyclotron, either on-site or, at minimum, very nearby. The exception to this is ^{82}Rb, as this positron-emitter can be produced with an on-site ^{82}Sr/^{82}Rb generator (the half-life of ^{82}Sr is 25.36 days).

Apart from ^{18}F, the positron-emitters that are most commonly used in cardiac PET are ^{13}N, ^{15}O, ^{82}Rb, and ^{11}C. Once generated, the positron-emitters are incorporated into tracers by a radiopharmacist. The myocardial kinetics of a given tracer will reflect the metabolism of an endogenous substrate of interest and, hence, can be used to glean information regarding the cellular pathways followed by that substrate. Further, with the aid of attenuation correction algorithms, the absolute quantities of a given tracer can be measured, allowing the quantification of regional myocardial blood flow and metabolic rates for the handling of a variety of physiologically important tracers. In the case of FDG, the concentration of this tracer following a peripheral intravenous injection can be used to estimate the rate of glucose utilization. ^{13}N labeled NH_3, ^{15}O labeled H_2O, and ^{82}Rb are valuable tracers for estimating myocardial perfusion.[121]

Measuring Glucose Uptake with ^{18}F-labeled FDG PET

FDG is transported into the cell by the same sarcolemmal carrier as glucose, where it is quickly phosphorylated to FDG-6-phosphate by the enzyme, hexokinase. This unidirectional reaction results in the intracellular accumulation of FDG-6-phosphate, as there is no phosphatase that can otherwise facilitate the dephosphorylation of FDG-6-phosphate and allow free FDG to exit the cell. Since FDG does not undergo further metabolism, its uptake is proportional to the overall rate of trans-sarcolemmal transport and hexokinase phosphorylation of circulating glucose by the myocardium.[122]

Historically, FDG PET has been used to assess fasting glucose utilization,[122] or that which occurs after oral glucose loading.[123] More recently, FDG imaging protocols have used the euglycemic hyperinsulinemic clamp technique: a constant infusion of glucose and insulin is initiated and the rate of glucose infusion adjusted to obtain normal blood glucose levels (verified by serial blood sampling). This protocol results in a post-absorptive "steady state," and is a means of circumventing problems related to insulin resistance and stimulating maximal FDG uptake.[124,125]

As there should be no uptake of glucose by infarcted myocardium—which is metabolically inert—nonviable myocardium will appear as a region of low-FDG concentration in such images. However, glucose utilization is normal and even above normal in areas of reversibly injured myocardium.[126–128] Thus, stunned or hibernating myocardium may be indistinguishable from normal tissue in an FDG PET image. Although fatty acid oxidation stops shortly after the onset of severe ischemia, the ischemic myocytes will derive energy from stored glycogen through anaerobic glycolysis. After glycogen stores have been depleted, the ischemic myocyte can make extremely efficient use of its meager supply of circulating glucose. Even under conditions of extremely diminished glucose delivery, there is evidence that certain sarcolemmal glucose transporters are up-regulated to allow for increased uptake of this substrate.[129] Upon successful reperfusion, it has been shown that the once-ischemic myocytes revert quickly to fatty-acid oxidation as their predominant source of HEP.[130]

A 1997 meta-analysis of data pooled from 11 FDG PET studies reported a combined sensitivity and specificity of 88 and 73%, respectively, for predicting functional recovery post-revascularization.[131] It should be added that, since that particular review appeared in print, at least two studies have reported worse specificities for this technique (33%[57] and 56%[58]). In the article by Wiggers et al., it was suggested that the specificity of FDG PET could be improved with the addition of perfusion imaging.

Myocardial Perfusion Imaging with $^{13}NH_3$, $H_2{}^{15}O$, and ^{82}Rb

$^{13}NH_3$, $H_2{}^{15}O$, and ^{82}Rb are the tracers most commonly used in PET perfusion imaging. Their

extremely short half-lives (10 min for ^{13}N, 2.03 min for ^{15}O, and 1.25 min for ^{82}Rb) permit repeat measurements, later in the same imaging exam which is extremely advantageous when calculating perfusion reserve (the ratio of maximum flow during exercise or pharmacologic stress to resting flow). Estimations of myocardial perfusion performed with $^{13}NH_3$ and $H_2{}^{15}O$ PET have compared very favorably with radiolabeled microsphere measurements (in animals), over a wide-range of flow values.[132] Although its initial uptake is in proportion to myocardial blood flow, the *retention* of $^{13}NH_3$ is thought to depend on the metabolic integrity of the myocytes. That is, once in the cell, $^{13}NH_3$ and glutamic acid are converted to ^{13}N-labeled glutamine, which is an ATP dependent reaction. Thus, late-distribution $^{13}NH_3$ PET images may also prove useful in the assessment of myocardial viability.[133,134]

Like ^{201}Tl, ^{82}Rb is a potassium analog whose uptake is initially proportional to perfusion. PET imaging with ^{82}Rb is an attractive alternative to $^{13}NH_3$ or $H_2{}^{15}O$ imaging since no cyclotron facility is required to generate ^{82}Rb. Rather, ^{82}Rb can be obtained as needed from a $^{82}Sr/^{82}Rb$ generator. Myocardial perfusion estimation by ^{82}Rb PET has been successfully performed in dogs and it has demonstrated good agreement with radiolabeled-microsphere measurements of perfusion.[135,136] As with Tl-201 SPECT imaging, ^{82}Rb has value beyond that of a perfusion tracer, as it is also believed that late-distribution ^{82}Rb images reflect myocardial viability as the successful uptake of ^{82}Rb depends on an intact myocyte membrane (a functional Na^+/K^+ ATPase pump).[137]

The Combined Value of Perfusion/Metabolism PET

The evaluation of tissue viability with either PET—or any other modality for that matter—is greatly improved with the concurrent assessment of regional myocardial perfusion. Thus, using FDG imaging, the classical picture of viability is the perfusion/glucose uptake mismatch, i.e., impaired perfusion with normal or augmented glucose uptake.

The combination of perfusion PET and FDG PET has long been considered the gold-standard for the identification of hibernating myocardium; the identification of a region with low perfusion reserve by $^{13}NH_3$ despite normal FDG uptake is highly predictive of both functional recovery[138,139] and survival[140,141] post-revascularization. In terms of soft post-operative outcomes, a significant correlation has been found between the total extent of PET mismatch and percent improvement in functional status post-revascularization.[142] To further this point, a separate study showed that the degree of improvement in exercise capacity could be predicted by the extent of viable myocardium identified by PET perfusion/metabolism testing, but not with dobutamine-echocardiography.[8]

Due to the relatively high cost and poor availability of PET, there is a real need to prove that PET confers superior prognostic impact, particularly relative to SPECT. In perhaps the only such study of this kind, an analysis of patient outcomes following either perfusion/metabolism PET or Tc-99m-sestamibi SPECT found no difference between the two techniques, in terms of either patient management (revascularization or drug treatment) or cardiac event-free survival.[143] It is notable, however, that this particular study involved few patients (35%) with severe LV dysfunction—a sub-population that is arguably the most likely to require aggressive management. Clearly, this remains an important question begging further study, ideally in the form of larger-scale trials.

Investigating Oxidative Metabolism with PET

Although changes in myocardial glucose utilization can be determined with FDG, this tracer provides no information regarding *how* substrate is utilized (i.e., oxidative metabolism vs. anaerobic glycolysis). This is an important distinction, as the ability to resume and maintain oxidative metabolism is an important predictor of subsequent functional recovery.[144,145] The extent and location of oxidative metabolism can be determined with ^{11}C-acetate PET, a technique that was first examined in dogs by Buxton and colleagues.[146] The PET imaging following ^{11}C-acetate injection allows for the subsequent measurement of myocardial CO_2 production, and is therefore directly related to tricarboxylic acid cycle flux.[147] This technique has been compared with FDG PET in patients with chronic CAD.[148] Although the difference was not significant, in this 1993 study by Gropler et al., ^{11}C-acetate tended to show superior predictive value, in terms of anticipating functional recovery post-revascularization. Additionally, since the initial uptake of ^{11}C-acetate is in direct relation to blood flow, it has been argued that ^{11}C-acetate PET may one day replace dual perfusion/metabolic imaging with $^{13}NH_3/^{18}FDG$.[149]

Combining PET-Tracers with SPECT Technology

Despite its proven value in the assessment of CAD, the high cost of PET imaging has precluded its widespread use in cardiac imaging. In contrast, the

relative availability of SPECT systems has fueled recent efforts to modify SPECT hardware for use in FDG imaging. Two approaches have been proposed for FDG imaging with modified-SPECT. The first involves the use of 511 keV collimators, so-called "ultra-high energy" (UHE) SPECT. The more recent alternative, gamma-camera coincidence imaging (GCD), involves double- or triple-detector gamma-cameras from which the collimators have been removed and the two 511 keV photons are detected using coincidence electronics (added to the conventional SPECT system).

Hasegawa and colleagues discussed the relative strengths and weaknesses of PET, UHE-SPECT, and GCD imaging (all with FDG) in a recent article.[150] With FDG PET set as the gold standard for the detection of myocardial viability, UHE-SPECT achieved a sensitivity and specificity of 67 and 92%, respectively. Though GCD imaging was comparable in terms of specificity (94%), its sensitivity was highly dependent on attenuation: with attenuation correction, GCD achieved a sensitivity of 48% but, without such correction, its sensitivity dropped to less than 19%. Attenuation was, intuitively, not as much of a concern with the single-detector UHE approach, as only one 511 keV photon would need to pass through the body before hitting the detector (versus two photons with the coincidence imaging approach).[151] The poor sensitivity of GCD was still somewhat surprising, as this technique conferred much better count sensitivity than did UHE SPECT. In terms of spatial resolution, GCD imaging was superior to UHE SPECT: the in-plane resolution of the former was reportedly 4.8 mm (FWHM, only slightly worse than that achievable by PET) compared to 9.2 mm for the latter. GCD fared much better in a clinical pilot study comparing it with FDG PET.[152] The sensitivity and specificity of GCD for the detection of myocardial viability (as determined by FDG PET) were evaluated at 81 and 69%, respectively. Furthermore, GCD demonstrated 79% agreement with PET in this study of patients with previous AMI.

Given that (1) the diagnostic accuracy of GCD and UHE SPECT techniques is in fact worse than that of true PET systems, (2) the cost of basic PET systems has become more competitive, and, finally, (3) given the proven need of PET in oncology, it is unlikely, in our opinion, that this technology will see widespread use.

Magnetic Resonance

Myocardial stunning is difficult to prove in the clinical setting, as one must establish that the dysfunction persists after the restoration of normal perfusion. Confirming the presence of hibernating myocardium also poses a challenge: the dysfunction must be ascribed to chronic hypoperfusion, chronically sub-normal perfusion reserve, or repetitive stunning. The noninvasive methods that are currently available for assessing perfusion generally lack the ability to resolve transmural variations in viability. PET, Tl-201, Tc-99m-sestamibi SPECT, and even MCE cannot identify differences in perfusion, metabolic patterns, and membrane integrity in subendocardial vs. subepicardial regions. As well, these techniques struggle to provide registered and concurrent measurements of perfusion and regional contractile function, two extremely important clinical parameters.

Magnetic resonance imaging (MRI) is rapidly gaining recognition as a highly versatile cardiac imaging tool in the setting of CAD. In addition to myocardial perfusion and contractile function, cardiac magnetic resonance (MR) techniques are also capable of assessing myocardial metabolism and coronary artery anatomy. In the following section, an attempt will be made to review the wide variety of MR techniques that have been developed to assess myocardial viability.

P-31 MR Spectroscopic Imaging

^{31}P MR spectroscopic imaging (^{31}P MRSI) has been used to observe the metabolic changes that accompany both ischemia and reperfusion. Briefly, cardiac ^{31}P MRSI is performed by placing a radio-frequency (RF) surface-coil over the apex of the heart (in vitro or in vivo, over the chest wall), and acquiring spatially localized ^{31}P spectra from the myocardium. The spectra corresponding to the voxels of interest, those in the LV blood-pool and myocardium, contain detailed information regarding phosphorous-containing compounds. The relative concentrations of HEP and inorganic phosphate can be ascertained from these spectra by integrating or numerically fitting the spectra in the time or frequency domain. Unfortunately, the inferior regions of the heart are inaccessible, in vivo, with this technique, due to the limitations of surface-receive coils that are commonly used in ^{31}P MRSI.[153]

^{31}P MRSI is a noninvasive alternative to myocardial biopsy—PET and spectroscopy being the only practical alternatives available for assessing myocardial metabolism.[154] As discussed earlier, it is well known that ATP falls drastically after the onset of acute ischemia. Ischemic yet viable myocardium loses PCr as well, and such changes have been observed with ^{31}P MRSI.[155] The normal ratio of PCr/ATP in humans is approxi-

mately 1.8.[156] ^{31}P MRSI has been applied to the study of stunned myocardium. Specifically, the relative PCr/β-ATP ratio was determined in patients undergoing early reperfusion for AMI. Although the ratio of these compounds was not seen to change over a period of 39 days post-AMI, it was concluded that the diminished concentration of both PCr and ATP lead to the relative stability of this metabolic ratio in stunned myocardium.[154] An alternative explanation, however, may be that the technique's limited spatial resolution did not allow for the discrimination of a characteristic pattern for infarct vs. peri-infarct ischemic but viable myocardium. At present, it is believed that ATP levels are within normal limits in hibernating myocardium.[157]

Additionally, one can determine intracellular pH by measuring the chemical shift (spectral separation) between the PCr and inorganic-phosphate peaks. Intracellular pH is known to fall during acute ischemia and it has been shown to return to normal following restoration of normal flow, even in regions with documented irreversible injury. It would thus, appear that pH cannot be used as a surrogate indicator of viability.

Diminished concentrations of PCr and ATP are not highly specific for ischemic injury or nonviability. Patients with cardiac allografts, patients undergoing adriamycin therapy, and those with cardiomyopathy or advanced age may demonstrate these metabolic abnormalities as well.[158] Perhaps the most promising application of ^{31}P MRSI is in the evaluation of patients with microvascular CAD—those with chest pain but without angiographic evidence of significant epicardial stenoses. Using mild exercise (isometric handgrip) stress, Buchtal and colleagues have demonstrated that a decrease in the PCr/ATP ratio can be used as a metabolic marker for ischemia in women with chest pain not secondary to an obstruction in one of the major epicardial coronary arteries.[159] This and other forms of the ^{31}P NMR stress test[160] may prove especially valuable in understanding the metabolic consequences of microvascular CAD and their contribution to LV dysfunction in certain groups of cardiac patients.

As mentioned earlier, ^{31}P MRSI is limited by poor spatial resolution at conventional field-strengths: at 1.5 T, the average voxel size interrogated by ^{31}P MRSI is on the order of 25 cm^3. This is problematic, as neighboring liver or skeletal muscle from the chest wall may contaminate the myocardial HEP peaks. Since liver has no PCr and skeletal muscle has relatively high concentrations of PCr, the magnitude of this partial volume contamination may be considerable. Hetherington and colleagues have acquired ^{31}P MRSI spectra of the human heart at higher field, 4.1 T, in order to improve the spatial resolution (to 8 cm^3) and thus, minimize the occurrence of such partial volume artifacts.[161] Despite these attempts, at present, there does not appear to be a distinctive "metabolic signature" for ischemic but viable myocardium obtained with magnetic resonance spectroscopy.

MR Imaging

^{1}H MRI can confer very high spatial resolution, on the order of sub-mm^2 to 2 mm^2 (in-plane resolution). This is important, as was discussed in the prelude to this section: without the capacity to distinguish transmural variations in viability, conventional imaging techniques are ill-equipped to accurately define the extent of necrosis, which could lead to either underestimation or overestimation of viability.

In the early days of cardiac MRI, basic spin–echo (SE) images were the mainstay, as they were easily acquired and provided high soft-tissue contrast. In SE images, there is no signal detected from flowing blood, leading to the appearance of "black blood" in the ventricles.[162] The first cardiac MR protocols usually included a T_2-weighted SE sequence, as it was quickly discovered that distinctions between infarcted and normal tissue were best seen with images of this type. In canine[163–169] and porcine[170] models of AMI, as well as in the earliest cardiac MRI experiments with patients,[171] T_2-weighted SE sequences allowed for the visualization of infarcted myocardium, which appears as a region of increased signal intensity ("hyperenhanced" region).

The first attempts to either measure T_1 (e.g., with inversion recovery sequences) or to acquire T_1-weighted SE images revealed that the T_1 of infarcted myocardium was distinctly prolonged compared to normal myocardium, resulting in regions of decreased signal intensity ("hypoenhanced" regions).[163–169,172] Attempts to identify areas of purely reversible ischemic injury were somewhat less encouraging: using a canine model of short-term occlusion followed by reperfusion, McNamara and colleagues found no differences between reversibly damaged and normal myocardium, in terms of either T_1 or T_2-based signal intensity.[173] T_2-weighted SE still finds a place in modern cardiac MRI, although conventional SE has been largely replaced by turbo SE.[174,175] Gradient-recalled-echo (GRE) sequences grew increasingly popular in cardiac

MRI, as GRE images can be acquired in less time than is required by SE sequences. However, GRE images confer less soft-tissue contrast than that which is possible with SE. In addition, unlike SE images, flowing blood appears bright on GRE images.[162] Modern cardiac sequences are largely GRE-based, including those developed for the assessment of myocardial perfusion and contractile-function, which will be discussed next.

Cine MRI: Assessment of Left-Ventricular Function

Cine MRI enables the visualization of cardiac motion in a manner similar to echocardiography and, thus, is a valuable tool for the assessment of viability. Of course, echocardiography is already equipped to handle *real-time* imaging of cardiac motion; it is also substantially cheaper and more widely available than cine MRI examinations. The advantage of cine MRI for the evaluation of LV function is its superior delineation of endocardial borders. As mentioned in the discussion regarding echocardiography, poor endocardial border definition can manifest in rather inaccurate estimations of regional wall thickening, %WT or ejection fraction, EF%. Cine MR images are generally of much better quality and therefore easier to interpret and can be quantified much more accurately and consistently than the echocardiographic equivalents (and thus, less dependent on the skill and training of the interpreting physician).

The additional value of pharmacologic stress (e.g., dobutamine) has made it possible to evaluate contractile reserve with cine MRI.[60,123,176] Dobutamine stress-cine MRI can be used to determine inotropic changes in both systolic and diastolic function. In an important study by Baer and colleagues, the sensitivity and specificity of dobutamine-induced systolic wall-thickening, as determined by cine MRI were 88 and 87%, respectively (when using FDG PET, in itself not ideal, as the standard).[123] Furthermore, dobutamine stress-cine MRI has been successful in the prediction of recovery following revascularization procedures: dobutamine stress-cine MRI measurements made before and 4–6 months post-revascularization revealed a sensitivity and specificity of 89 and 94%, respectively, for functional improvement.[177] More recently, Oshinski et al. applied a relatively simple mathematical model for use in predicting changes in global function (EF%) with revascularization. By combining their model with pre-intervention cine MRI data acquired from patients with chronic LV dysfunction, it was possible to predict the actual post-revascularization ejection fraction within 1.3 EF percentage points.[178]

There is evidence suggesting that cine MRI may be able to assess LV function for patients with inadequate acoustic windows.[176] In a study of 208 patients, Nagel et al. compared dobutamine-echocardiography and dobutamine cine MRI. Only 51% of the echocardiograms were considered to be of good or very good image quality, whereas fully 82% of the MR equivalents were graded that highly.[179] It is particularly noteworthy that 70% of the echocardiograms in this study were acquired with second-harmonic techniques, which optimize endocardial definition.

A limitation that is common to both echocardiography and conventional cine MRI is that neither can provide the radial or circumferential components of cardiac motion. The addition of "grid-tagging" has improved on conventional cine-MRI by providing a means of calculating radial and circumferential deformation of the myocardium. Grid-tagging sequences involve the application of a pre-saturation grid at the beginning of the cardiac cycle: this appears as a null-signal grid-pattern (fiducial markers) that can be used to follow intramyocardial changes in contractility.[180,181] In a recent study, cine MRI with grid tagging was used to assess the three-dimensional nature of contractile dysfunction in a canine model of stunned myocardium.[182]

Contrast-Enhanced MRI

It can be said that the introduction of paramagnetic contrast agents truly inspired the notion of the comprehensive cardiac MRI exam. Cine MRI, on its own, is insufficient for discriminating between reversible and irreversible ischemic injury. Without a means of assessing myocardial perfusion and/or membrane integrity, the impetus to develop MR techniques for clinical use was poor.

Gd-DTPA is the most widely available and tested MR contrast agent. It is a freely diffusible, extracellular tracer with a molecular size of 550 Da. This tracer results in contrast enhancement by reducing the T_1 of tissue in a concentration dependent fashion. Although free Gd^{3+} is toxic, when chelated to DTPA, the tracer has an excellent safety profile and clearance is predominantly via glomerular filtration. The chelator, DTPA, is the moiety responsible for the distribution and kinetics of the whole tracer: healthy cells (with intact, selectively permeable cell membranes) will exclude Gd-DTPA and therefore

this agent is restricted to the extravascular and interstitial spaces.[183,184]

Without contrast enhancement, distinctions between normal and infarcted myocardium were unclear when based on T_1 differences alone. T_2-weighted SE allowed for the visualization of infarcted tissue, without the aid of contrast media, but the specificity of either increased signal intensity or measured T_2 for irreversible injury was questionable. The areas of signal increase often extended well beyond the histologically determined infarct zones, suggesting a strong influence of peri-infarct edema on the images. Early applications of contrast enhanced MRI demonstrated considerable improvement in T_1-based contrast between infarcted and normal myocardium.[185,186] The heightened sensitivity of T_1-weighted imaging with Gd-DTPA was ascribed to the T_1-shortening properties of the agent, although Gd-DTPA also reduces T_2 (to a lesser extent). The increased concentration of Gd-DTPA in infarcted regions is thought to be caused by the loss of membrane integrity in irreversibly injured myocytes: the contrast agent can begin to enter the extravascular intra-cellular space and, hence, increase its volume of distribution. This excess accumulation of Gd-DTPA in infarcted (hypo-perfused) vs. normally perfused tissue may be further encouraged by delayed washout kinetics of the tracer due to sub-optimal venous drainage in these areas.[187] There will be an expanded discussion of the application of Gd-DTPA for infarct assessment in the forthcoming sections.

Myocardial Perfusion Imaging

A comprehensive assessment of myocardial viability should include an assessment of perfusion. Determining the presence of an intact microvasculature can help to discriminate between ischemic (but viable) and infarcted myocardium. Like nuclear medicine SPECT and PET imaging, MRI can be used for the study of myocardial perfusion. With the aid of rapid GRE sequences, MRI can be used to qualitatively assess regional blood flow by monitoring the first-pass of a bolus of contrast agent, e.g., Gd-DTPA. Regions that fail to enhance during first pass are served by critically stenosed coronary vessels with associated perfusion defects.[188–193] Tracer kinetic modeling can be applied to these images to estimate tissue parameters such as perfusion, blood volume, and both membrane and capillary permeability.

A useful addition to MR perfusion imaging is the use of vasodilators. By comparing perfusion with and without adenosine-induced vasodilation, for example, one can arrive at an estimate of perfusion reserve. Perfusion reserve may be helpful in the detection of significant stenoses as it is been determined that flow during maximum hyperemia reaches nearly 400% of resting flow, in normal subjects[194] and is reduced progressively for stenoses greater than 50%. This may also eventually serve to distinguish stunned myocardium from either hibernating or infarcted tissue. In dogs, coronary blood flow autoregulation is normal in stunned tissue, as it will respond to vasodilatory stimuli (e.g., exogenous adenosine) to the same extent as will normal tissue.[195] Despite its functional similarity to stunned tissue, hibernating myocardium is characterized by depressed coronary perfusion reserve (as previously discussed). It should be emphasized that techniques for identifying and quantifying perfusion reserve should be capable of detecting small (2-fold) regional differences in flow to be of real clinical value. To address this challenge, Klocke et al. have tested the performance of an inversion-recovery prepared TrueFISP sequence in a series of canine, first-pass adenosine-stress experiments.[196] With the signal-to-noise, dynamic range, and temporal resolution provided by this sequence, it was possible to discriminate regional depressions in vasodilated flow over a rather wide range (1–5 times baseline flow). Dipyridamole stress MRI was recently compared with dipyridamole stress Tl-201 SPECT, in a small study of patients with single-vessel CAD.[197] There was modest agreement between the two modalities; the sensitivity and specificity of MRI in the detection of Tl-201 identified perfusion defects were 71 and 71%, respectively.

Perfusion imaging is certainly an active area of cardiac MR research but, it is also one that is fraught with many unresolved issues, from those relating to hardware requirements, to those concerning the prudent choice of contrast-medium, MR pulse-sequence, and tracer-kinetic model. For a more extensive discussion pertaining to MRI perfusion imaging of the heart, the reader is directed to an excellent review by Canet et al.[198]

Delayed Enhancement Patterns

"Delayed imaging," performed several minutes after a bolus injection of contrast-agent provides a simple approach to the assessment of myocardial viability. Approximately 10–20 min after the injection of the bolus, infarcted tissue will manifest as regions of hyperenhancement. Several groups have adopted this approach; to date, delayed hyperenhancement studies have been performed on rats (acute/reperfused[199–204]

and chronic/unreperfused models,[204]) dogs (acute/reperfused[205–209] and chronic/unreperfused[208,209]), and on human subjects (patients with either reperfused AMI[210–213] or chronic disease[214–219]). Among the studies that performed delayed enhancement imaging on patients scheduled for PTCA or CABG, cine MRI was used to assess functional recovery at approximately 3[215,216] or 6 months[218] post-revascularization. Using this approach, delayed enhancement imaging has emerged as the most popular MRI approach used clinically. After a bolus injection, the signal enhancement changes depend on both regional myocardial blood flow and the distribution volume of the contrast agent.[205,206,220] To this point, Lauerma et al. recently demonstrated that the convenience of late-enhancement imaging (10 min after the bolus injection) was offset by a serious penalty in sensitivity, for segmental improvement in LV function, when compared with a combination exam of dobutamine-stress MR and first-pass enhancement kinetic modeling (62% for late-enhancement vs. 97% for cine MR and first-pass imaging, in detecting irreversible myocardial defects).[218] Further, in the delayed enhancement approach, where imaging is performed at a fixed time period after bolus injection, it is assumed that the tracer kinetics for both washin and washout are similar in all settings, i.e., sustained coronary occlusion with markedly reduced residual blood flow vs. reperfused infarcts with normal or near normal blood flow. This data is not as yet available.

Having said that, this simple technique allows detection of even small infarcts. In a study by Ricciardi et al., infarcts of 2 g on average were detected clinically by delayed contrast enhanced imaging.[221] Wu et al. also demonstrated the ability to identify both Q wave and non-Q wave infarcts at 3 and 14 months following acute occlusion.[217] Choi and colleagues have pursued the logical extension of this work by investigating the relationship between MRI-determined infarct size (transmural extent) and long-term functional improvement.[212] In this compelling study, the authors demonstrated that the size of the dysfunctional but normally enhancing region (1 week after the acute event) was the single best predictor of functional recovery 8–12 weeks post-reperfusion. As for the prognostic impact on patients not revascularized, Klein and colleagues demonstrated that the sensitivity and specificity of delayed hyperenhancement for detecting either transmural or nontransmural scar tissue (as defined by $^{13}NH_3/^{18}FDG$ PET mismatch) were 83 and 88%, respectively.[219]

Although it has been thought that only infarcted cells lose cell membrane integrity and cease to prevent intracellular entry of this tracer, Saeed and colleagues have demonstrated, in rats, that Gd-DTPA enhanced regions were 33% larger than the extent of infarcts identified by triphenyltetrazolium chloride (TTC) staining at day 2.[202] However, in this study, data was obtained 24 hr after infarction, and this may have not allowed sufficient time for the effects of apoptosis to develop. Fieno et al., studying a canine model, did not find overestimation of infarct size, demonstrating an r value of 0.95 between either in vivo or ex vivo enhanced images vs. TTC staining.[209]

An alternative approach to Gd-DTPA enhancement is to immediately follow the bolus-injection by a constant-infusion of the contrast agent. In this manner, equilibrium concentrations of the tracer can be achieved in the tissue, thus making it possible to estimate the distribution volume or partition coefficient (λ) of Gd-DTPA in mL/g.[186] Assuming normal renal clearance, an optimum constant infusion dose can be chosen such that [Gd-DTPA] will reach equilibrium in ($\leq$15 min, in all but the most severely ischemic regions of myocardium (perfusion $<$0.05 mL/min/g), provided that the permeability surface-area product of permanently damaged myocytes is similar to that of capillaries.[222] This is an assumption that has been recently brought into question.[223]

As discussed earlier, Gd-DTPA can begin to enter the formerly intracellular space if the sarcolemma breaks down. Loss of sarcolemmal integrity is a defining characteristic of irreversible injury. Thus, it seemed reasonable to postulate that the λ in infarcted myocardium would exceed that of normal tissue and, in fact, it has been shown to be more than double that of normal myocardium (0.8 vs. 0.3 mL/g).[186,224,225] In order to validate the constant-infusion approach in the setting of unreperfused infarction, Pereira and colleagues also estimated the λ in dogs with chronic left anterior descending (LAD) coronary artery occlusion. It was determined that the increase in λ in infarcted tissue could be seen after 2 days and for at least 3 weeks following occlusion. The authors concluded that λ is elevated in infarcted tissue, regardless of reperfusion status.[226]

Recently, this technique has been applied to patients with acutely reperfused AMI. This clinical study demonstrated that λ was inversely correlated to areas of low count-density on resting Tl-201 images.[227] Flacke and coworkers have further demonstrated that the λ of gadopentetate dimeglumine, also determined during a constant infusion, can be used to differentiate between normal and infarcted myocardium in patients with either acute or chronic myocardial infarction.[228]

Clearly, what then remained to be shown was whether this increase in λ was specific to infarcted myocardium.

To address the issue of the change in enhancement pattern with reversible injury, the partition coefficient of Gd-DTPA was evaluated in canines subjected to 30 min severe coronary occlusion followed by over 3 weeks reperfusion.[229] The results of this work demonstrated that λ in stunned myocardium was not elevated above that of normal tissue at any time point or in any animal studied. Tl-201 uptake measurements served to confirm the preservation of myocardial viability. Serial measurements of regional LV function via cine MRI provided the evidence of prolonged yet reversible contractile dysfunction that is phenotypic of myocardial stunning.

Given the results described here and those reported by previous studies of infarcted myocardium,[225] it is now reasonable to conclude that increases in the signal enhancement of Gd-DTPA, with either delayed enhancement imaging or following a constant infusion, are specific to myocardium that has sustained irreversible injury. A summary of our current understanding of the relationship between myocardial viability and the distribution of Gd-DTPA is shown in Fig. 1. When used in conjunction with cine MRI assessments of contractility, this MRI protocol could be used to determine the existence and extent of normal, stunned, and infarcted myocardium, as follows.

1. Viable tissue (normal or reversibly damaged) vs. nonviable tissue can be discriminated based on differences in λ or signal intensity; both stunned and infarcted tissue will exhibit contractile dysfunction, so a distinction cannot be based on a cine MRI assessment alone.
2. Normal vs. reversibly ischemic tissue can be discriminated based on differences in regional contractile function, as assessed by cine MRI; as normal and stunned tissue will demonstrate similar signal, a distinction cannot be based on contrast-enhancement alone.

Early work towards the assessment of Gd-DTPA distribution in hibernating tissue has shown that λ is normal in areas served by a chronically stenosed (80%) branch of the LAD, despite significant hypoperfusion and depressed global ventricular function (EF%).[230]

In the emergency room setting, delineation of acute infarction from old scar or myocardial fibrosis associated with pre-existing conditions (e.g., cardiomyopathies) is needed. Quantification of signal intensity or the associated volume of distribution shows promise in the distinction between acute infarct and chronic scar and may also identify fibrosis due to cardiomyopathies based

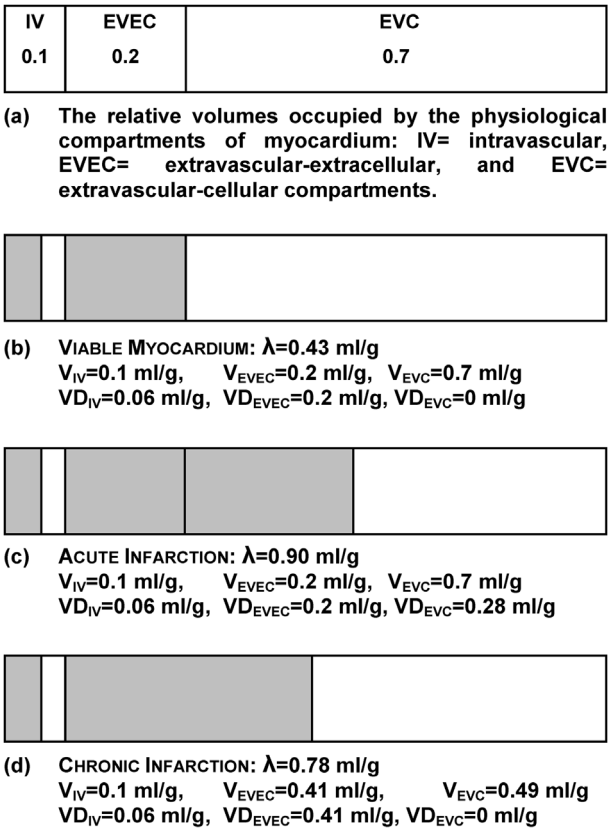

Figure 1. If the myocardial physiological compartments shown in (a) are assumed to be 0.1 mL/g for the intravascular volume (V_{IV}), 0.2 mL/g for the extravascular-extracellular volume (V_{EVEC}), and 0.7 mL/g for the extravascular-cellular volume (V_{EVC}), then the observed partition-coefficients, λ, in viable (b), acutely infarcted (c), and chronically infarcted (d) myocardium can be understood as volumes of distribution (VD) of Gd-DTPA. In viable myocardium with $\lambda = 0.43\,\mathrm{mL/g}$ and a hematocrit of 0.4, the VD for V_{IV} would be 0.06 mL/g, the VD for V_{EVEC} would be 0.20 mL/g and the VD for V_{EVC} would be zero. In acutely infarcted myocardium, λ can increase to 0.9 mL/g if 0.28 mL/g of V_{EVC} can dissolve Gd-DTPA with the same concentration as it can in plasma. In chronically infarcted myocardium (scar), λ has been measured by Flacke et al.[228] to be 0.78 mL/g. The remodeling process results in a net decrease in V_{EVC}: despite the appearance of (viable) myofibroblasts, there is a concomitant loss of myocytes. The physiological compartment sizes which would result in a $\lambda = 0.78\,\mathrm{mL/g}$ (for a hematocrit of 0.4) are shown in (d). Here, it has been assumed that Gd-DTPA cannot permeate the membranes of the viable, cellular components of old scar.

on distinctive alterations in signal intensity or distribution volume.[231–233]

Na-23 and Rb-87 MR Imaging

Cannon and colleagues first attempted to obtain ^{23}Na MR images of ischemic myocardium in 1987, when it was hypothesized that the increased intracellular [Na^+] that develops with acute infarction could be exploited to identify regions of irreversibly injured myocardium.[234] This proposal met with skepticism and was deemed wildly impractical, in large part due to the very poor MR sensitivity of sodium (approximately 1/4 that of proton). Nevertheless, this novel approach to viability imaging was later adopted and adapted by Kim et al., using rabbit[235] and canine[236] models of acute reperfused infarction. These animal studies supported the earlier reports of a strong relationship between increased signal intensity on ^{23}Na MR images and irreversible damage, since there were no increases in image signal intensity in either normal or reversibly injured regions. Although preliminary ^{23}Na MR images may look disappointing in terms of spatial-resolution, the use of high field systems (>3 T) or innovations in sodium MR pulse-sequence design may serve to establish a place for ^{23}Na MR imaging in the noninvasive assessment of myocardial viability.

In addition to the diminished capacity to remove intracellular Na^+ that occurs with prolonged ischemia, the disruption of the Na^+/K^+ ATPase dependent pump also manifests as reduced uptake of extracellular K^+. As previously discussed, potassium analogs such as Rb-82 and Tl-201 are used extensively in nuclear medicine based cardiac imaging as both perfusion and viability tracers. As well, another Rubidium isotope, ^{87}Rb has been used to generate MR maps of potassium flux because its MR sensitivity is far higher than that of ^{39}K. Kupriyanov and colleagues have successfully used ^{87}Rb MR imaging to demonstrate the reduction in potassium flux that accompanies ischemia, in an isolated pig heart model.[237] After tracer-kinetic modeling and image analysis, the ^{87}Rb content in infarcted regions was estimated to be 40% of its baseline content. It thus seemed a logical next step to evaluate possible correlations between ^{23}Na and ^{87}Rb MR image intensity in the same model of infarction. As would be expected, the interleaved acquisition of ^{23}Na and ^{87}Rb MR images revealed areas of reduced ^{87}Rb intensity that corresponded to regions of *increased* ^{23}Na intensity, in the same isolated pig heart preparation.[238] Taken together, the ratio of ^{23}Na to ^{87}Rb in infarcted tissue was a more sensitive indicator of irreversible injury than either technique used in isolation.

SUMMARY: VALUE OF CURRENT IMAGING TECHNIQUES

Now that the relative merits of several cardiac imaging techniques have been described, it is perhaps appropriate to make some general statements regarding the assessment of myocardial viability. With very few exceptions, all of the techniques discussed are reasonably sensitive and therefore capable of detecting irreversible injury where it exists, particularly when the necrosis extends through the full thickness of myocardium. It is more often the case that conventional diagnostic testing lacks specificity and thus, cannot provide the clinician with a means of separating viable—yet stunned or hibernating—myocardium from that which is nonviable.

Given the profound cellular adaptations that occur during hibernation, it is not surprising that contractile reserve may not always be present in hibernating myocardium, as it is for stunned myocardium. For this reason, inotropic stress testing (e.g., dobutamine-echocardiography) may be inadequate, on its own, for the prediction of functional recovery post-revascularization.[239] The diagnostic accuracy of our noninvasive assessment should be enhanced by our ability to interrogate the metabolic or membrane function of the tissue. At present, the gold standard test for the identification of hibernating myocardium is the combined $^{13}NH_3/^{18}FDG$ PET exam. A region of low flow that demonstrates high FDG uptake is considered highly predictive of functional recovery, post-revascularization.[138]

The transmural heterogeneity of injury continues to be relatively difficult to determine with the current spatial resolution of conventional PET imaging technology ($\sim$6 mm full width at half maximum.[240]) With the technologies currently available, no *one* test is used to guide the full course of patient management. The combination of cine MRI and contrast-enhanced MRI with Gd-DTPA is quickly gaining popularity in the cardiac imaging community. More clinical evaluations are needed, however, in order to evaluate the true sensitivity and specificity of MR techniques for the prediction of functional recovery and prognosis improvement in CAD patients. A more pressing need is to evaluate the MR contrast-enhancement characteristics of hibernating tissue *itself*.

Hibernation, though clinically well recognized, is extremely difficult to model in experimental settings. This is due, in large part, to the difficulty associated with maintaining a *chronic* stenosis that does not result in any *irreversible* injury. Most early models of "hibernation" were not truly representative of the chronic, clinical situation. Later attempts to maintain stenoses over the course of several weeks were also fraught with problems, as the long-term hypoperfusion often resulted in small areas of necrosis.[54]

While we have endeavored to emphasize the relative strengths and weaknesses of the techniques discussed in this review, there are several factors that complicate a rigorous comparison between or among imaging modalities. This is particularly important whenever metrics like sensitivity or specificity are cited. A given gold-standard is chosen primarily because it has passed the test of time. Although it is difficult to argue with the firm, historical pedigree of conventional coronary angiography, echocardiography, or nuclear medicine techniques, it is clear that newer technologies like second-harmonic MCE and MRI will play increasingly important roles as they become more thoroughly evaluated.

It goes without saying that there will be ongoing differences in the apparent delineation of viability, or infarct extent, when one modality is compared against another. Differences between perfusion vs. cellular membrane integrity, vs. preserved but altered myocardial metabolism, vs. systolic and diastolic function should be expected, as each technique examines different cellular or vascular functions. Even the instruments used to assess these are often affected by a variety of different mechanisms. For example, all perfusion tracers are delivered to myocardium in direct proportion to flow, but depend on cellular membrane functions to sequester them within the myocardial cells. Therefore, their distribution is not only purely a reflection of flow, but also of the status of metabolic integrity of a given region, and may therefore be reduced in the setting of stunned and hibernating myocardium.

Further, of vital importance is to put the abstract concept of determination of viability with diagnostic techniques into clinical relevance. In the era of evidence-based medicine, the choice of viability test is necessarily related to its cost-effectiveness. Ultimately, each of these imaging tests will have to prove their worth with demonstrable effects on clinical outcomes: longer event-free survival and improved quality of life. The viability test that promises the greatest impact on these outcomes for a limited amount of health care resources is, by definition, the most cost-effective choice. Recently, several large clinical trials have been undertaken to assess the effects of thrombolytic therapy for the management of AMI. These have reported 30-day mortality rates of 6–7%. However, patients participating in clinical trials are not necessarily representative of the general population of patients they are purported to exemplify. In 1999, a comprehensive audit was undertaken in Ontario, Canada to review the mortality rates for all patients hospitalized with a diagnosis of myocardial infarction.[241] The 30 day mortality averaged 15% and, at 1 year, 23%. These very high rates reflect the magnitude of the remaining problem. Cardiac deaths are directly related to impairment of LV systolic function. Improvement in LV function is likely associated with a proportional improvement in prognosis. Our ability to accurately diagnose and treat reversible dysfunction will lead to a significant lessening of the mortality and morbidity associated with AMI.

REFERENCES

1. Luciani, G.B.; Montalbano, G.; Casali, G.; Mazzucco, A. Prediciting Long-Term Functional Results After Myocardial Revascularization in Ischemic Cardiomyopathy. J. Thorac. Cardiovasc. Surg. **2000**, *120*, 478–489.
2. Alfieri, O. Coronary Artery Bypass Grafting for Left Ventricular Dysfunction. Curr. Opin. Cardiol. **1994**, *9*, 658–663.
3. Maddahi, J.; Schelbert, H.; Brunken, R.; Di Carli, M. Role of Thallium-201 and PET Imaging in Evaluation of Myocardial Viability and Management of Patients with Coronary Artery Disease and Left Ventricular Dysfunction. J. Nucl. Med. **1994**, *35*, 707–715.
4. Di Carli, M.F.; Davidson, M.; Little, R.; Khanna, S.; Mody, F.V.; Brunken, R.C.; Czernin, J.; Rokhsar, S.; Stevenson, L.W.; Laks, H. Value of Metabolic Imaging with Positron Emission Tomography for Evaluating Prognosis in Patients with Coronary Artery Disease and Left Ventricular Dysfunction. Am. J. Cardiol. **1994**, *73*, 527–533.
5. Shapira, I.; Heller, I.; Pines, A.; Topilsky, M.; Isakov, A. The Impact of Myocardial Viability as Determined by Rest-Redistribution ^{201}Tl Single Photon Emission CT Imaging and The Choice of Therapy on Prognosis in Patients with Left Ventricular Dysfunction. J. Med. **2000**, *31*, 205–214.
6. Chikamori, T.; Hirose, K.; Hamada, T.; Hitomi, N.; Kitaoka, H.; Yabe, T.; Furono, T.; Seo, H.; Yamashiro, T.; Doi, Y. Functional Recovery After Coronary Artery Bypass Grafting in Patients with Severe Left Ventricular Dysfunction and Preserved Myocardial Viability in the

Left Anterior Descending Arterial Territory as Assessed by Thallium-201 Myocardial Perfusion Imaging. Jpn. Circ. J. **1999**, *63*, 752–758.
7. Moore, R.W.; Noe, S.; Carvalho, J., Jr.; Balingit, A.; Taylor, A.J. Rest-Distribution 201-Tl Single-Photon Emission CT Imaging for Determination of Myocardial Viability: Relationship Among Viability, Mode of Therapy, and Long-Term Prognosis. Chest **1999**, *115*, 1621–1626.
8. Marwick, T.H.; Zuchowski, C.; Lauer, M.S.; Secknus, M.A.; Williams, J.; Lytle, B.W. Functional Status and Quality of Life in Patients with Heart Failure Undergoing Coronary Bypass Surgery After Assessment of Myocardial Viability. J. Am. Coll. Cardiol. **1999**, *33*, 750–758.
9. Pagano, D.; Townend, J.N.; Littler, W.A.; Horton, R.; Camici, P.G.; Bonser, R.S. Coronary Artery Bypass Surgery as Treatment for Ischemic Heart Failure: The Predictive Value of Viability Assessment with Quantitative Positron Emission Tomography for Symptomatic and Functional Outcome. J. Thorac. Cardiovasc. Surg. **1998**, *115*, 791–799.
10. Senior, R.; Kaul, S.; Lahiri, A. Myocardial Viability on Echocardiography Predicts Long-Term Survival After Revascularization in Patients with Ischemic Congestive Heart Failure. J. Am. Coll. Cardiol. **1999**, *33*, 1848–1854.
11. Reimer, K.A.; Jennings, R.B.; Tatum, A.H. Pathobiology of Acute Myocardial Ischemia: Metabolic, Functional and Ultrastructural Studies. Am. J. Cardiol. **1983**, *52*, 72A–81A.
12. Jennings, R.B.; Schaper, J.; Hill, M.L.; Steenbergen, C.; Reimer, K.A. Effect of Reperfusion Late in the Phase of Reversible Ischemic Injury: Changes in Cell Volume, Electrolytes, Metabolites, and Ultrastructure. Circ. Res. **1985**, *56*, 262–278.
13. Schoen, F.J. The Heart. In *Pathologic Basis of Disease*; Cotran, R.S., Kumar, V., Collins, T., Eds.; W.B. Saunders: Philadelphia, 1999; 544–556.
14. Cotran, R.S.; Kumar, V.; Collins, T. Cellular Pathology I: Cell Injury and Cell Death. In *Pathologic Basis of Disease*; Cotran, R.S., Kumar, V., Collins, T., Eds.; W.B. Saunders: Philadelphia, 1999; 15–16.
15. Bartling, B.; Holtz, J.; Darmer, D. Contribution of Myocyte Apoptosis to Myocardial Infarction? Basic. Res. Cardiol. **1998**, *93*, 71–84.
16. Elsässer, A.; Suzuki, K.; Lorenz-Meyer, S.; Bode, C.; Schaper, J. The Role of Apoptosis in Myocardial Ischemia: A Critical Appraisal. Basic. Res. Cardiol. **2001**, *96*, 219–226.
17. Bonow, R.O. Identification of Viable Myocardium. Circulation **1996**, *94*, 2674–2680.
18. Reimer, K.A.; Lowe, J.E.; Rasmussen, M.M.; Jennings, R.B. The Wavefront Phenomenon of Ischemic Cell Death: 1. Myocardial Infarct Size vs. Duration of Coronary Occlusion in Dogs. Circulation **1977**, *56* (5), 786–793.
19. Higgins, C.B. Prediction of Myocardial Viability by MRI. Circulation **1999**, *99*, 727–729.
20. Heyndrickx, G.R.; Millard, R.W.; McRitchie, R.J.; Maroko, P.R.; Vatner, S.F. Regional Myocardial Functional and Electrophysiological Alterations After Brief Coronary Artery Occlusion in Conscious Dogs. J. Clin. Invest. **1975**, *56*, 978–985.
21. Braunwald, E.; Kloner, R.A. The Stunned Myocardium: Prolonged, Post-Ischemic Ventricular Dysfunction. Circulation **1982**, *66*, 1146–1149.
22. Rahimtoola, S.H. A Perspective on the Three Large Multicenter Randomized Clinical Trials of Coronary Artery Bypass Surgery for Chronic Stable Angina. Circulation **1985**, *72* (Suppl. V), V123–V135.
23. Rahimtoola, S.H. From Coronary Artery Disease to Heart Failure: Role of Hibernating Myocardium. Am. J. Cardiol. **1995**, *75*, 16e–22e.
24. Vanoverschelde, J.-L.J.; Wijns, W.; Borgers, M.; Heyndrickx, G.; Depré, C.; Flameng, W.; Melin, J.A. Chronic Myocardial Hibernation in Humans: From Bedside to Bench. Circulation **1997**, *95*, 1961–1971.
25. Nixon, J.V.; Brown, C.N.; Smitherman, T.C. Identification of Transient and Persistent Segmental Wall Motion Abnormalities in Patients with Unstable Angina by Two-dimensional Echocardiography. Circulation **1982**, *65*, 1497–1503.
26. Kloner, R.A.; Allen, J.; Cox, T.A.; Zheng, Y.; Ruiz, C.E. Stunned Left Ventricular Myocardium Following Exercise Treadmill Testing in Coronary Artery Disease. Am. J. Cardiol. **1991**, *68*, 329–334.
27. Breisblatt, W.M.; Stein, K.L.; Wolfe, C.J.; Follansbee, W.P.; Capozzi, J.; Armitage, J.M.; Hardesty, R.L. Acute Myocardial Dysfunction and Recovery: A Common Occurrence After Coronary Bypass Surgery. J. Am. Coll. Cardiol. **1990**, *15*, 1261–1269.
28. Touchstone, D.A.; Beller, G.A.; Nygaard, T.W.; Tedesco, C.; Karl, S. Effects of Successful Intravenous Reperfusion Therapy on Regional Myocardial Function and Geometry in Humans: A Tomographic Assessment Using Two-Dimensional Echocardiography. J. Am. Coll. Cardiol. **1989**, *13*, 1506–1513.
29. Barnes, E.; Baker, C.S.R.; Dutka, D.P.; Rimoldi, O.; Rinaldi, C.A.; Nihoyannopoulos, P.; Camici, P.G.; Hall, R.J.C. Prolonged Left Ventricular Dysfunction Occurs in Patients with Coronary Artery Disease After Both Dobutamine and Exercise Induced Myocardial Ischaemia. Heart **2000**, *83*, 283–289.
30. Keeble, W.; Martin, W.; Hutton, I. Myocardial Stunning After Streptokinase: What is the Significance of the Q Wave? Heart **2000**, *83*, e11.
31. Bolli, R.; Zhu, W.X.; Thornby, J.I.; O'Neill, P.G.; Roberts, R. Time Course and Determinants of Recovery

of Function After Reversible Ischemia in Conscious Dogs. Am. J. Physiol. **1988**, *254*, H102–H114.
32. Kloner, R.A.; Bolli, R.; Marban, E.; Reinlib, L.; Braunwald, E.; and Participants in the NHLBI Workshop. The Medical and Cellular Implications of Myocardial Stunning, Hibernation, and Preconditioning. Circulation **1998**, *97*, 1848–1867.
33. Puri, P.S. Correlation Between Biochemical and Contractile Changes After Myocardial Ischemia and Revascularization. Recent. Adv. Stud. Cardiac. Struct. Metab. **1975**, *7*, 161–169.
34. Eberli, F.R.; Weinberg, E.O.; Grice, W.N.; Horowitz, G.L.; Apstein, C.S. Protective Effect of Increased Glycolytic Substrate Against Systolic and Diastolic Dysfunction and Increased Coronary Resistance from Prolonged Global Underperfusion and Reperfusion in Isolated Rabbit Hearts Perfused with Erythrocyte Suspensions. Circ. Res. **1991**, *68*, 468–481.
35. Owen, P.; Dennis, S.; Opie, L.H. Glucose Flux Rate Regulates Onset of Ischemic Contracture in Globally Underperfused Rat Hearts. Circ. Res. **1990**, *66*, 344–354.
36. Braasch, W.; Gudbjarnason, S.; Puri, P.S.; Ravens, K.G.; Bing, R.J. Early Changes in Energy Metabolism in the Myocardium Following Acute Coronary Artery Occlusion in Anaesthetized Dogs. Circ. Res. **1968**, *23*, 429–438.
37. DeBoer, L.V.W.; Ingwall, J.S.; Kloner, R.A.; Braunwald, E. Prolonged Derangements of Canine Myocardial Purine Metabolism After a Brief Coronary Artery Occlusion Not Associated with Anatomic Evidence of Necrosis. Proc. Natl Acad. Sci. **1980**, *77*, 5471–5475.
38. Ellis, S.G.; Henschke, C.I.; Sandor, T.; Wynne, J.; Braunwald, E.; Kloner, R.A. Time Course of Functional and Biochemical Recovery of Myocardium Salvaged by Reperfusion. J. Am. Coll. Cardiol. **1983**, *1*, 1047–1055.
39. Weiss, J.; Hiltbrand, B. Functional Compartmentation of Glycolytic versus Oxidative Metabolism in Isolated Rabbit Heart. J. Clin. Invest. **1985**, *82*, 723–735.
40. Gao, W.D.; Atar, D.; Backx, P.H.; Marban, E. Relationship Between Intracellular Calcium and Contractile Force in Stunned Myocardium: Direct Evidence for Decreased Myofilament Ca^{2+} Responsiveness and Altered Diastolic Function in Intact Ventricular Muscle. Circ. Res. **1995**, *76*, 1036–1048.
41. Van Eyk, J.E.; Powers, F.; Law, W.; Larue, C.; Hodges, R.S.; Solaro, R.J. Breakdown and Release of Myofilament Proteins During Ischemia and Ischemia/reperfusion in Rat Hearts: Identification of Degradation Products and Effects on the pCa-Force Relation. Circ. Res. **1998**, *82*, 261–271.
42. Foster, D.B.; Van Eyk, J.E. In Search of the Proteins That Cause Myocardial Stunning. Circ. Res. **1999**, *85*, 470–472.
43. Gao, W.D.; Atar, D.; Liu, Y.; Perez, N.G.; Murphy, A.M.; Marban, E. Role of Troponin I Proteolysis in the Pathogenesis of Stunned Myocardium. Circ. Res. **1997**, *80*, 393–399.
44. McDonough, J.L.; Arrell, D.K.; Van Eyk, J.E. Troponin I Degradation and Covalent Complex Formation Accompanies Myocardial Ischemia/Reperfusion Injury. Circ. Res. **1999**, *84*, 9–20.
45. Murphy, A.M.; Kogler, H.; Georgakopoulos, D.; McDonough, J.L.; Kass, D.A.; Van Eyk, J.E.; Marban, E. Transgenic Mouse Model of Stunned Myocardium. Science **2000**, *287*, 488–491.
46. Li, X.Y.; McCay, P.B.; Zughaib, M.; Jeroudi, M.O.; Triana, J.F.; Bolli, R. Demonstration of Free Radical Generation in the "Stunned" Myocardium in the Conscious Dog and Identification of Major Differences Between Conscious and Open-Chest Dogs. J. Clin. Invest. **1993**, *92*, 1025–1041.
47. Bolli, R.; Marban, E. Molecular and Cellular Mechanisms of Myocardial Stunning. Physiol. Rev. **1999**, *79* (2), 609–634.
48. Casey, T.M.; Arthur, P.G. Hibernation in Noncontracting Mammalian Cardiomyocytes. Circulation **2000**, *102*, 3124–3129.
49. Uren, N.G.; Melin, J.A.; De Bruyne, B.; Wijns, W.; Baudhuin, T.; Camici, P.G. Relation Between Myocardial Blood Flow and the Severity of Coronary-Artery Stenosis. N. Engl. J. Med. **1994**, *330*, 1782–1788.
50. Pagano, D.; Fath-Ordoubadi, F.; Beatt, K.J.; Townend, J.N.; Bonser, R.S.; Camici, P.G. Effects of Coronary Revascularisation on Myocardial Blood Flow and Coronary Vasodilator Reserve in Hibernating Myocardium. Heart **2001**, *85*, 208–212.
51. Ausma, J.; Cleutjens, J.; Thone, F.; Flameng, W.; Ramaekers, F.; Borgers, M. Chronic Hibernating Myocardium: Interstitial Changes. Mol. Cell. Biochem. **1995**, *147*, 35–42.
52. Ausma, J.; Schaart, G.; Thone, F.; Shivalkar, B.; Flameng, W.; Depré, C.; Vanoverschelde, J.L.; Ramaekers, F.; Borgers, M. Chronic Ischemic Viable Myocardium in Man: Aspects of De-differentiation. Cardiovasc. Pathol. **1995**, *4*, 29–37.
53. Camici, P.G.; Wijns, W.; Borgers, M.; DeSilva, R.; Ferrari, R.; Knutti, J.; Lammertsma, A.A.; Liedtke, A.J.; Paternostro, G.; Vatner, S.F. Pathophysiological Mechanisms of Chronic Reversible Left Ventricular Dysfunction Due to Coronary Artery Disease (Hibernating Myocardium). Circulation **1997**, *96*, 3205–3214.
54. Elsässer, A.; Schlepper, M.; Klövekorn, W.-P.; Cai, W.-J.; Zimmermann, R.; Müller, K.-D.; Strasser, R.; Kostin, S.; Gagel, C.; Münkel, B.; Schaper, W.; Schaper, J. Hibernating Myocardium: An Incomplete Adaptation to Ischemia. Circulation **1997**, *96*, 2920–2931.

55. Rahimtoola, S.H. Hibernating Myocardium Has Reduced Blood Flow at Rest That Increases with Low-Dose Dobutamine. Circulation **1996**, *94*, 3055–3061.
56. Nagueh, S.F.; Mikati, I.; Weilbaecher, D.; Reardon, M.J.; Al-Zaghrini, G.J.; Cacela, D.; He, Z.-X.; Letsou, G.; Noon, G.; Howell, J.F.; Espada, R.; Verani, M.S.; Zoghbi, W.A. Relation of the Contractile Reserve of Hibernating Myocardium to Myocardial Structure in Humans. Circulation **1999**, *100*, 490–496.
57. Pagano, D.; Bonser, R.S.; Townend, J.N.; Ordoubadi, F.; Lorenzoni, R.; Camici, P.G. Predictive Value of Dobutamine Echocardiography and Positron Emission Tomography in Identifying Hibernating Myocardium in Patients with Postischemic Heart Failure. Heart **1998**, *79*, 281–288.
58. Wiggers, H.; Nielsen, T.T.; Bottcher, M.; Egeblad, H.; Botker, H.E. Positron Emission Tomography and Low-Dose Dobutamine Echocardiography in the Prediction of Postrevascularization Improvement in Left Ventricular Function and Exercise Parameters. Am. Heart. J. **2000**, *140*, 928–936.
59. Hoffman, R.; Lethen, H.; Marwick, T.; Arnese, M.; Fioretti, P.; Pingitore, A.; Picano, E.; Buck, T.; Erbel, R.; Flachskampf, F.A.; Hanrath, P. Analysis of Interinstitutional Observer Agreement in Interpretation of Dobutamine Stress Echocardiograms. J. Am. Coll. Cardiol. **1996**, *27*, 330–336.
60. Hundley, W.G.; Hamilton, C.A.; Thomas, M.S.; Herrington, D.M.; Salido, T.B.; Kitzman, D.W.; Little, W.C.; Link, K.M. Utility of Fast Cine Magnetic Resonance Imaging and Display for the Detection of Myocardial Ischemia in Patients Not Well Suited for Second Harmonic Stress Echocardiography. Circulation **1999**, *100*, 1697–1702.
61. Kasprzak, J.D.; Paelinck, B.; Ten Cate, F.J.; Vletter, W.B.; de Jong, N.; Poldermans, D.; Elhendy, A.; Bouakaz, A.; Roelandt, J.R. Comparison of Native and Contrast-Enhanced Harmonic Echocardiography for Visualization of Left Ventricular Endocardial Border. Am. J. Cardiol. **1999**, *83*, 211–217.
62. Espinola-Zavaleta, N.; Vargas-Barron, J.; Romero-Cardenas, A.; Bialostozky, D.; Alexanderson, E.; Martinez-Sanchez, C.; Pena-Duque, M.; Keirns, C.; Rijlaarsdam, M.; Lupi-Herrera, E. Multiplane Transesophageal Echocardiography with Dobutamine in Patients with Biventricular Inferior Myocardial Infarction. Echocardiography **1998**, *15*, 181–190.
63. Baer, F.M.; Theissen, P.; Crnac, J.; Schmidt, M.; Deutsch, H.J.; Sechtem, U.; Schicha, H.; Erdmann, E. Head to Head Comparison of Dobutamine-transoesophageal Echocardiography and Dobutamine-magnetic Resonance Imaging for the Prediction of Left Ventricular Functional Recovery in Patients with Chronic Coronary Artery Disease. Eur. Heart. J. **2000**, *21*, 981–991.
64. Caidahl, K.; Kazzam, E.; Lidberg, J.; Neumann, A.; Andersen, G.; Nordanstig, J.; Rantapaa, C.; Dahlqvist, S.; Waldenstrom, A.; Wikh, R. New Concept in Echocardiography: Harmonic Imaging of Tissue Without the Use of Contrast Agent. Lancet **1998**, *352*, 1264–1270.
65. Monaghan, M.J. Second Harmonic Imaging: A New Tune for an Old Fiddle? Heart **2000**, *83*, 131–132.
66. Franke, A.; Hoffmann, R.; Kuhl, H.P.; Lepper, W.; Breithardt, O.A.; Schormann, M.; Hanrath, P. Noncontrast Second Harmonic Imaging Improves Interobserver Agreement and Accuracy of Dobutamine Stress Echocardiography in Patients with Impaired Image Quality. Heart **2000**, *83*, 133–140.
67. Burns, P.N. Harmonic Imaging with Ultrasound Contrast Agents. Clin. Radiol. **1996**, *51*, 50–55.
68. Firschke, C.; Lindner, J.R.; Wei, K.; Goodman, N.C.; Skyba, D.M.; Kaul, S. Myocardial Perfusion Imaging in the Setting of Coronary Artery Stenosis and Acute Myocardial Infarction Using Venous Injection of a Second-Generation Echocardiographic Contrast Agent. Circulation **1997**, *96*, 959–967.
69. Wei, K.; Jayaweera, A.R.; Firoozan, S.; Linka, A.; Skyba, D.M.; Kaul, S. Quantification of Myocardial Blood Flow with Ultrasound-Induced Destruction of Microbubbles Administered as a Constant Venous Infusion. Circulation **1998**, *97*, 473–483.
70. Lepper, W.; Hoffmann, R.; Kamp, O.; Franke, A.; de Cock, C.C.; Kuhl, H.P.; Sieswerda, G.T.; vom Dahl, J.; Janssens, U.; Voci, P.; Visser, C.A.; Hanrath, P. Assessment of Myocardial Reperfusion by Intravenous Myocardial Contrast Echocardiography and Coronary Flow Reserve After Primary Percutaneous Transluminal Coronary Angiography in Patients with Acute Myocardial Infarction. Circulation **2000**, *101*, 2368–2374.
71. Ito, H.; Iwakura, K.; Oh, H.; Masuyama, T.; Hori, M.; Higashino, Y.; Fujii, K.; Minamino, T. Temporal Changes in Myocardial Perfusion Patterns in Patients with Reperfused Anterior Wall Myocardial Infarction. Their Relation to Myocardial Viability. Circulation **1995**, *91*, 656–662.
72. Brochet, E.; Czitrom, D.; Karila-Cohen, D.; Seknadji, P.; Faraggi, M.; Benamer, H.; Aubry, P.; Steg, P.G.; Assayag, P. Early Changes in Myocardial Perfusion Patterns After Myocardial Infarction: Relation with Contractile Reserve and Functional Recovery. J. Am. Coll. Cardiol. **1998**, *32*, 2011–2017.
73. Meza, M.F.; Kates, M.A.; Barbee, W.; Revall, S.; Perry, B.; Murgo, J.P.; Cheirif, J. Combination of Dobutamine and Myocardial Contrast Echocardiography to Differentiate Postischemic From Infarcted Myocardium. J. Am. Coll. Cardiol. **1997**, *29*, 974–984.
74. Agrawal, G.; Cape, E.G.; Raichlen, J.S.; Tirtaman, C.; Lee, E.T.; Fan, P.H.; Nanda, N.C. Usefulness of Combined Color Doppler/Contrast in Providing

Complete Delineation of Left Ventricular Cavity. Am. J. Cardiol. **1997**, *80*, 98–101.
75. Kornbluth, M.; Liang, D.H.; Brown, P.; Gessford, E.; Schnittger, I. Contrast Echocardiography is Superior to Tissue Harmonics for Assessment of Left Ventricular Function in Mechanically Ventilated Patients. Am. Heart. J. **2000**, *140*, 291–296.
76. Pohost, G.M.; Zir, L.M.; Moore, R.H.; McKusick, K.A.; Guiney, T.E.; Beller, G.A. Differentiation of Transiently Ischemic from Infarcted Myocardium by Serial Imaging After a Single Dose of Thallium-201. Circulation **1977**, *55*, 294–302.
77. Gibson, R.S.; Watson, D.D.; Craddock, G.B.; Crampton, R.S.; Kaiser, D.L.; Denny, M.J.; Beller, G.A. Prediction of Cardiac Events After Uncomplicated Myocardial Infarction: A Prospective Study Comparing Predischarge Exercise Thallium-201 Scintigraphy and Coronary Angiography. Circulation **1983**, *68*, 321–336.
78. Zimmermann, R.; Mall, G.; Rauch, B.; Zimmer, G.; Gabel, M.; Zehelein, J.; Bubeck, B.; Tillmanns, H.; Hagl, S.; Kübler, W. Residual ^{201}Tl Activity in Irreversible Defects as a Marker of Myocardial Viability: Clinicopathological Study. Circulation **1995**, *91*, 1016–1021.
79. Gibbons, R.J. Myocardial Perfusion Imaging. Heart **2000**, *83*, 355–360.
80. Yang, L.D.; Berman, D.S.; Kiat, H.; Resser, K.J.; Friedman, J.D.; Rozanski, A.; Maddahi, J. The Frequency of Late Reversibility in SPECT Thallium-201 Stress-Redistribution Studies. J. Am. Coll. Cardiol. **1989**, *15*, 334–340.
81. de Sutter, J.; U/nderwood, R. Prognostic Implications of Infarct Size Assessed by Myocardial Perfusion Single-Photon Emission Tomography. Eur. J. Nucl. Med. **2000**, *27*, 269–272.
82. Dilsizian, V.; Rocco, T.P.; Freedman, N.M.; Leon, M.B.; Bonow, R.O. Enhanced Detection of Ischemic but Viable Myocardium by the Reinjection of Thallium After Stress-Redistribution Imaging. N. Engl. J. Med. **1990**, *323*, 141–146.
83. Rocco, T.P.; Dilsizian, V.; McKusick, K.A.; Fischman, A.J.; Boucher, C.A.; Strauss, H.W. Comparison of Thallium Redistribution with Rest "Reinjection" Imaging for the Detection of Viable Myocardium. Am. J. Cardiol. **1990**, *66*, 158–163.
84. Perrone-Filardi, P.; Chiarello, M.; Underwood, R. The Assessment of Myocardial Viability and Hibernation Using Resting Thallium Imaging. Clin. Cardiol. **2000**, *23*, 719–722.
85. Castini, D.; Bestetti, A.; Garbin, M.; Di Leo, C.; Bigi, R.; Sonzilli, C.; Concardi, G.; Gioventu, M.; Tarolo, G.L.; Lombardi, F.; Fiorenti, C. Myocardial Viability Assessment After Acute Myocardial Infarction: Low-Dose Dobutamine Echocardiography Versus Rest-Redistribution Thallium-201 SPECT. Cardiologia **1999**, *44*, 817–823.
86. Amanullah, A.M.; Chaudhry, F.A.; Heo, J.; Galatro, K.; Dourdoufis, P.; Brozena, S.; Narula, J.; Iskandrian, A.E. Comparison of Dobutamine Echocardiography, Dobutamine Sestamibi, and Rest-Redistribution Thallium-201 Single-Photon Emission Computed Tomography for Determining Contractile Reserve and Myocardial Ischemia in Ischemic Cardiomyopathy. Am. J. Cardiol. **1999**, *84*, 626–631.
87. Gunning, M.G.; Angnostopoulos, C.; Davies, G.; Knight, C.J.; Pennell, D.J.; Fox, K.M.; Pepper, J.; Underwood, S.R. Simultaneous Assessment of Myocardial Viability and Function for the Detection of Hibernating Myocardium Using ECG-Gated ^{99m}Tc-tetrofosmin Emission Tomography: A Comparison with ^{201}Tl Emission Tomography Combined with Cine Magnetic Resonance Imaging. Nucl. Med. Commun. **1999**, *20*, 209–214.
88. Pace, L.; Perrone-Filardi, P.; Storto, G.; Della Morte, A.M.; Dellegrottaglie, S.; Prastaro, M.; Crisci, T.; Ponticelli, M.P.; Piscione, F.; Chiariello, M.; Salvatore, M. Prediction of Improvement in Global Left Ventricular Function in Patients with Chronic Coronary Artery Disease and Impaired Left Ventricular Function: Rest Thallium-201 SPET versus Low-Dose Dobutamine Echocardiography. Eur. J. Nucl. Med. **2000**, *27*, 1740–1746.
89. Pace, L.; Perrone-Filardi, P.; Mainenti, P.; Cuocolo, A.; Vezzuto, P.; Prastaro, M.; Varrone, A.; De Luca, G.; Soricelli, A.; Betocchi, S.; Chiariello, M.; Salvatore, M. Identification of Viable Myocardium in Patients with Chronic Coronary Artery Disease Using Rest-Redistribution Thallium-201 Tomography: Optimal Image Analysis. J. Nucl. Med. **1998**, *39*, 1869–1874.
90. Piwnica-Worms, D.; Kronauge, J.F.; Delmon, L.; Holman, B.L.; Marsh, J.D.; Jones, A.G. Effect of Metabolic Inhibition on Technetium-99m-MIBI Kinetics in Cultured Chick Myocardial Cells. J. Nucl. Med. **1990**, *31*, 464–472.
91. Maurea, S.; Cuocolo, A.; Soricelli, A.; Castelli, L.; Nappi, A.; Squame, F.; Imbriaco, M.; Trimarco, B.; Salvatore, M. Enhanced Detection of Viable Myocardium by Technetium-99m-MIBI Imaging After Nitrate Administration in Chronic Coronary Artery Disease. J. Nucl. Med. **1995**, *36*, 1945–1952.
92. Schneider, C.A.; Voth, E.; Gawlitch, S.; Baer, F.M.; Horst, M.; Schicha, H.; Erdmann, E.; Sechtem, U. Significance of Rest Technetium-99m Sestamibi Imaging for the Prediction of Improvement of Left Ventricular Dysfunction After Q Wave Myocardial Infarction: Importance of Infarct Location Adjusted Thresholds. J. Am. Coll. Cardiol. **1998**, *32*, 648–654.
93. Batista, J.F.; Pereztol, O.; Valdes, J.A.; Sanchez, E.; Stusser, R.; Rochela, L.M.; Lopez, D.; Garcia, E.V.

Improved Detection of Myocardial Perfusion Reversibility by Rest-Nitroglycerin Tc-99m-MIBI: Comparison with Tl-201 Reinjection. J. Nucl. Cardiol. **1999**, *6*, 480–486.

94. Udelson, J.E.; Coleman, P.S.; Metherall, J.; Pandian, N.G.; Gomez, A.R.; Griffith, J.L.; Shea, N.L.; Oates, E.; Konstam, M.A. Predicting Recovery of Severe Regional Ventricular Dysfunction. Comparison of Resting Scintigraphy with 201-Thallium and ^{99m}Tc-Sestamibi. Circulation **1994**, *89*, 2552–2561.
95. Kaufmann, G.J.; Boyne, T.S.; Watson, D.D.; Smith, W.H.; Beller, G.A. Comparison of Rest Thallium-201 and Rest Technetium-99m Sestamibi Imaging for Assessment of Myocardial Viability in Patients with Coronary Artery Disease and Severe Left Ventricular Dysfunction. J. Am. Coll. Cardiol. **1996**, *27*, 1592–1597.
96. Soufer, R.; Dey, H.M.; Ng, C.K.; Zaret, B.L. Comparison of Sestamibi Single Photon Emission Computed Tomography to Positron Emission Tomography for Estimating Left Ventricular Myocardial Viability. Am. J. Cardiol. **1995**, *75*, 1214–1219.
97. Dilsizian, V.; Arrighi, J.A.; Diodati, J.G.; Quyyumi, A.A.; Alavi, K.; Bacharach, S.L.; Marin-Neto, J.A.; Katsiyiannis, P.T.; Bonow, R.O. Myocardial Viability in Patients with Chronic Coronary Artery Disease: Comparison of ^{99m}Tc-sestamibi with Thallium Reinjection and [18F]-Fluorodeoxyglucose. Circulation **1994**, *89*, 578–587.
98. Cuocolo, A.; Pace, L.; Ricciardelli, B.; Chiariello, M.; Trimarco, B.; Salvatore, M. Identification of Viable Myocardium in Patients with Chronic Coronary Artery Disease: Comparison of Thallium-201 Scintigraphy with Reinjection and Technetium-99m Methoxyisobutyl Isonitrile. J. Nucl. Med. **1992**, *33*, 505–511.
99. Hurrell, D.G.; Milavetz, J.; Hodge, D.O.; Gibbons, R.J. Infarct Size Determination by Technetium 99m Sestamibi Single-Photon Emission Computed Tomography Predicts Survival in Patients with Chronic Coronary Artery Disease. Am. Heart. J. **2000**, *140*, 61–66.
100. Platts, E.A.; North, T.L.; Pickett, R.D.; Kelly, J.D. Mechanism of Uptake of Technetium-Tetrofosmin. I: Uptake into Isolated Adult Rat Ventricular Myocytes and Subcellular Localization. J. Nucl. Med. **1995**, *2*, 317–326.
101. Younes, A.; Songadele, J.A.; Maublant, J.; Platts, E.A.; Pickett, R.D.; Veyre, A. Mechanism of Uptake of Technetium-Tetrofosmin. II: Uptake into Isolated Adult Rat Heart Mitochondria. J. Nucl. Med. **1995**, *2*, 327–333.
102. Kelly, J.D.; Forster, A.M.; Higley, B.; Archer, C.M.; Booker, F.S.; Canning, L.R.; Chiu, K.W.; Edwards, B.; Gill, H.K.; McPartlin, M.; Nagle, K.R.; Latham, I.A.; Pickett, R.D.; Storey, A.E.; Webbon, P.M. Technetium-99m-Tetrofosmin as a New Radiopharmaceutical for Myocardial Perfusion Imaging. J. Nucl. Med. **1993**, *34*, 222–227.
103. Sinusas, A.J.; Shi, Q.; Saltzberg, M.T.; Vitols, P.; Jain, D.; Wackers, F.J.; Zaret, B.L. Technetium-99m-Tetrofosmin to Assess Myocardial Blood Flow: Experimental Validation in an Intact Canine Model of Ischemia. J. Nucl. Med. **1994**, *35*, 664–671.
104. Glover, D.K.; Ruiz, M.; Yang, J.Y.; Smith, W.H.; Watson, D.D.; Beller, G.A. Myocardial ^{99m}Tc-Tetrofosmin Uptake During Adenosine-Induced Vasodilatation with Either a Critical or Mild Coronary Stenosis: Comparison with ^{201}Tl and Regional Myocardial Blood Flow. Circulation **1997**, *96*, 2332–2338.
105. Glover, D.K.; Ruiz, M.; Koplan, B.A.; Watson, D.D.; Beller, G.A. Assessment of Myocardial Perfusion and Viability with Technetium-99m-Tetrofosmin in Canine Models of Coronary Occlusion and Reperfusion. J. Nucl. Med. **1999**, *40*, 142–149.
106. Beller, G.A.; Zaret, B.L. Contributions of Nuclear Cardiology to Diagnosis and Prognosis of Patients with Coronary Artery Disease. Circulation **2000**, *101*, 1465–1478.
107. Pagley, P.R.; Beller, G.A.; Watson, D.D.; Gimple, L.W.; Ragosta, M. Improved Outcome After Coronary Artery Bypass Surgery in Patients with Ischemic Myopathy and Residual Myocardial Viability. Circulation **1997**, *96*, 793–800.
108. Brown, K.; Heller, G.; Landin, R.; Shaw, L.J.; Beller, G.A.; Pasquale, M.J.; Haber, S.B. Early Dipyridamole Technetium 99m Sestamibi Single Photon Emission Computed Tomographic Imaging 2 to 4 Days After Acute Myocardial Infarction Predicts In-Hospital and Post Discharge Cardiac Events. Circulation **1999**, *100*, 2060–2066.
109. Mahmarian, J.J.; Pratt, C.M.; Nishimura, S.; Abreu, A.; Verani, M.S. Quantitative Adenosine ^{201}Tl Single-Photon Emission Computed Tomography for the Early Assessment of Patients Surviving Acute Myocardial Infarction. Circulation **1993**, *87*, 1197–1210.
110. Zellweger, M.J.; Lewin, H.C.; Lai, S.; Dubois, E.A.; Friedman, J.D.; Germano, G.; Kang, X.; Sharir, T.; Berman, D.S. When to Stress Patients After Coronary Artery Bypass Surgery? Risk Stratification in Patients Early and Late Post-CABG Using Stress Myocardial Perfusion SPECT: Implications of Appropriate Clinical Outcome Strategies. J. Am. Coll. Cardiol. **2001**, *37*, 144–152.
111. Brown, K.A.; Rosman, D.R.; Dave, R.M. Stress Nuclear Myocardial Perfusion Imaging Versus Stress Echocardiography: Prognostic Comparisons. Prog. Cardiovasc. Dis. **2000**, *43*, 231–244.
112. Chee, N.K.; Batemen, T.M. Cost-Effectiveness of Stress Echocardiography and Nuclear Perfusion Imaging. Prog. Cardiovasc. Dis. **2000**, *43*, 197–214.

113. Hosokawa, R.; Nohara, R.; Fujibayashi, Y.; Okuda, K.; Ogino, M.; Hata, T.; Fujita, M.; Tamaki, N.; Konishi, J.; Sasayama, S. Myocardial Kinetics of Iodine-123-BMIPP in Canine Myocardium After Regional Ischemia and Reperfusion: Implications for Clinical SPECT. J. Nucl. Med. **1997**, *38*, 1857–1863.
114. Saraste, A.; Pulkki, K.; Kallajoki, M.; Henriksen, K.; Parvinen, M.; Voipio-Pulkki, L.-M. Apoptosis in Human Acute Myocardial Infarction. Circulation **1997**, *95*, 320–323.
115. Hofstra, L.; Liem, I.H.; Dumont, E.A.; Boersma, H.H.; van Heerde, W.L.; Doevendans, P.A.; DeMuinck, E.; Wellens, H.J.J.; Kemerink, G.J.; Reutelingsperger, C.P.M.; Heidendal, G.A. Visualisation of Cell Death In Vivo in Patients with Acute Myocardial Infarction. Lancet **2000**, *356*, 209–212.
116. van Heerde, W.L.; de Groot, P.G.; Reutelingsperger, C.P. The Complexity of the Phospholipid Binding Protein Annexin V. Thromb. Haemost. **1995**, *73*, 172–179.
117. Martin, S.J.; Finucane, D.M.; Amarante-Mendes, G.P.; O'Brien, G.A.; Green, D.R. Phosphatidylserine Externalization During Cd95-Induced Apoptosis of Cells and Cytoplasts Requires ICE/CED-3 Protease Activity. J. Biol. Chem. **1996**, *271*, 28753–28756.
118. Blankenberg, F.G.; Katsikis, P.D.; Tait, J.F.; Davis, R.E.; Naumovski, L.; Ohtsuki, K.; Kopiwoda, S.; Abrams, M.J.; Darkes, M.; Robbins, R.C.; Maecker, H.T.; Strauss, H.W. In Vivo Detection and Imaging of Phosphatidylserine Expression During Programmed Cell Death. Proc. Natl Acad. Sci. **1998**, *95*, 6349–6354.
119. De Sutter, J.; Lahorte, C.; Taeymans, Y.; Dierckx, R.; Slegers, G. Cell Death in Myocardial Infarction. Lancet **2000**, *356*, 1439–1440.
120. Bavelaar-Croon, C.D.L.; Kayser, H.W.M.; van der Wall, E.E.; de Roos, A.; Dibbets-Schneider, P.; Pauwels, E.K.J.; Germano, G.; Atsma, D.E. Left Ventricular Function: Correlation of Quantitative Gated SPECT and MR Imaging Over a Wide Range of Values. Radiology **2000**, *217*, 572–575.
121. Schelbert, H.R. Principles of Positron Emission Tomography. In *Cardiac Imaging*; Marcus, M.L., Schelbert, H.R., Skorton, D.J., Wolf, G.L., Eds.; W.B. Saunders: Philadelphia, 1991; 1140–1270.
122. Camici, P.G. Positron Emission Tomography and Myocardial Imaging. Heart **2000**, *83*, 475–480.
123. Baer, F.M.; Voth, E.; Schneider, C.A.; Theissen, P.; Schicha, H.; Sechtem, U. Comparison of Low-Dose Dobutamine-Gradient-Echo Magnetic Resonance Imaging and Positron Emission Tomography with [18F]Fluorodeoxyglucose in Patients with Chronic Coronary Artery Disease: A Functional and Morphological Approach to the Detection of Residual Myocardial Viability. Circulation **1995**, *91*, 1006–1015.
124. Shivalkar, B.; Maes, A.; Borgers, M.; Ausma, J.; Scheys, I.; Nuyts, J.; Mortelmans, L.; Flameng, W. Only Hibernating Myocardium Invariably Shows Early Recovery After Coronary Revascularization. Circulation **1996**, *94*, 308–315.
125. Fallavollita, J.A. Spatial Heterogeneity in Fasting and Insulin-Stimulated ^{18}F-2-deoxyglucose Uptake in Pigs with Hibernating Myocardium. Circulation **2000**, *102*, 908–914.
126. McNulty, P.H.; Jagasia, D.; Cline, G.W.; Ng, C.K.; Whiting, J.M.; Garg, P.; Shulman, G.I.; Soufer, R. Persistent Changes in Myocardial Glucose Metabolism In Vivo During Reperfusion of a Limited-Duration Coronary Occlusion. Circulation **2000**, *101*, 917–922.
127. Lopaschuk, G.D.; Stanley, W.C. Glucose Metabolism in the Ischemic Heart. Circulation **1997**, *95*, 313–315.
128. Depré, C.; Vanoverschelde, J.-L.J.; Taegtmeyer, H. Glucose for the Heart. Circulation **1999**, *99*, 578–588.
129. Young, L.H.; Renfu, Y.; Russel, R.; Hu, X.; Caplan, M.; Ren, J.; Shulman, G.I.; Sinusas, A.J. Low-Flow Ischemia Leads to Translocation of Canine Heart GLUT-4 and GLUT-1 Glucose Transporters to the Sarcolemma In Vivo. Circulation **1997**, *95*, 415–422.
130. Liedtke, A.J.; DeMaison, L.; Eggleston, A.M.; Cohen, L.M.; Nellis, S.H. Changes in Substrate Metabolism and Effects of Excess Free Fatty Acids in Reperfused Myocardium. Circ. Res. **1988**, *62*, 535–542.
131. Bax, J.J.; Wijns, W.; Cornel, J.H.; Visser, F.C.; Fioretti, P.M. Accuracy of Currently Available Techniques for Prediction of Functional Recovery After Revascularization in Patients with Left Ventricular Dysfunction Due to Chronic Coronary Artery Disease: Comparison of Pooled Data. J. Am. Coll. Cardiol. **1997**, *30*, 1451–1460.
132. De Silva, R.; Camici, P.G. The Role of Positron Emission Tomography in the Investigation of Coronary Circulatory Function in Man. Cardiovasc. Res. **1994**, *28*, 1595–1612.
133. Kitsiou, A.N.; Bacharach, S.L.; Bartlett, M.L.; Srinivasan, G.; Summers, R.M.; Quyyumi, A.A.; Dilsizian, V. ^{13}*N*-Ammonia Myocardial Blood Flow and Uptake: Relation to Functional Outcome of Asynergic Regions After Revascularization. J. Am. Coll. Cardiol. **1999**, *33*, 678–686.
134. Beanlands, R.S.B.; de Kemp, R.; Scheffel, A.; Nahmias, C.; Garnett, S.; Coates, G.; Johansen, H.L.; Fallen, E. Can Nitrogen-13 Ammonia Kinetic Modeling Define Myocardial Viability Independent of Fluorine-18 Fluorodeoxyglucose? J. Am. Coll. Cardiol. **1997**, *29*, 537–543.
135. Yoshida, K.; Mullani, N.; Gould, K.L. Coronary Flow and Flow Reserve by PET Simplified for Clinical Applications Using Rubidium-82 or Nitrogen-13-Ammonia. J. Nucl. Med. **1996**, *37*, 1701–1712.

136. de Kemp, R.A.; Ruddy, T.D.; Hewitt, T.; Dalipaj, M.M.; Beanlands, R.S.B. Detection of Serial Changes in Absolute Myocardial Perfusion with ^{82}Rb PET. J. Nucl. Med. **2000**, *41*, 1426–1435.
137. Gould, K.L.; Yoshida, K.; Hess, M.J.; Haynie, M.; Mullani, N.A.; Smalling, R.W. Myocardial Metabolism of Fluorodeoxyglucose Compared to Cell Membrane Integrity for the Potassium-Analogue Rubidium-82 for Assessing Infarct Size in Man by PET. J. Nucl. Med. **1991**, *32*, 1–9.
138. Tillisch, J.; Brunken, R.; Marshall, R.; Schwaiger, M.; Mandelkern, M.; Phelps, M.; Schelbert, H. Reversibility of Cardiac Wall Motion Abnormalities Predicted by Positron Emission Tomography. N. Engl. J. Med. **1986**, *314*, 884–888.
139. Depré, C.; Vanoverschelde, J.-L.J.; Gerber, B.; Borgers, M.; Melin, J.A.; Dion, R. Correlation of Functional Recovery with Myocardial Blood Flow, Glucose Uptake, and Morphologic Features in Patients with Chronic Left Ventricular Ischemic Dysfunction Undergoing Coronary Artery Bypass Grafting. J. Thorac. Cardiovasc. Surg. **1997**, *113*, 379–389.
140. Haas, F.; Haehnel, C.J.; Picker, W.; Nekolla, S.; Martinoff, S.; Meisner, H.; Schwaiger, M. Preoperative Positron Emission Tomographic Viability Assessment and Perioperative and Postoperative Risk in Patients with Advanced Ischemic Heart Disease. J. Am. Coll. Cardiol. **1997**, *30*, 1693–1700.
141. Di Carli, M.F.; Maddahi, J.; Rokhsar, S.; Schelbert, H.R.; Bianco-Batlles, D.; Brunken, R.C.; Fromm, B. Long-Term Survival of Patients with Coronary Artery Disease and Left Ventricular Dysfunction: Implications for the Role of Myocardial Viability Assessment in Management Decisions. J. Thorac. Cardiovasc. Surg. **1998**, *116*, 997–1004.
142. Di Carli, M.F.; Asgarzadie, F.; Schelbert, H.R.; Brunken, R.C.; Laks, H.; Phelps, M.E.; Maddahi, J. Quantitative Relation Between Myocardial Viability and Improvement in Heart Failure Symptoms After Revascularization in Patients with Ischemic Cardiomyopathy. Circulation **1995**, *92*, 3436–3444.
143. Siebelink, H.J.; Blanksma, P.K.; Crijns, H.J.G.M.; Bax, J.J.; van Boven, A.J.; Kingma, T.; Piers, D.A.; Pruim, J.; Jager, P.L.; Vaalburg, W.; van der Wall, E.E. No Difference in Cardiac Event-Free Survival Between Positron Emission Tomography-Guided and Single-Photon Emission Computed Tomography-Guided Patient Management: A Prospective, Randomized Comparison of Patients with Suspicion of Jeopardized Myocardium. J. Am. Coll. Cardiol. **2001**, *37*, 81–88.
144. Weinheimer, C.J.; Brown, M.A.; Nohara, R.; Perez, J.E.; Bergmann, S.R. Functional Recovery After Reperfusion Is Predicated on Recovery of Myocardial Oxidative Metabolism. Am. Heart. J. **1993**, *125*, 939–949.
145. Di Carli, M.F.; Prcevski, P.; Singh, T.P.; Janisse, J.; Ager, J.; Muzik, O.; Vander Heide, R. Myocardial Blood Flow, Function, and Metabolism in Repetitive Stunning. J. Nucl. Med. **2000**, *41*, 1227–1234.
146. Buxton, D.B.; Nienaber, C.A.; Luxen, A.; Ratib, O.; Hansen, H.; Phelps, M.E.; Schelbert, H.R. Noninvasive Quantitation of Regional Myocardial Oxygen Consumption In Vivo with [1-11C]Acetate and Dynamic Positron Emission Tomography. Circulation **1990**, *81*, 1594–1605.
147. Armbrecht, J.J.; Buxton, D.B.; Schelbert, H.R. Validation of [1-11C]Acetate as a Tracer for Noninvasive Assessment of Oxidative Metabolism with Positron Emission Tomography in Normal, Ischemic, Postischemic, and Hyperemic Canine Myocardium. Circulation **1990**, *81*, 1594–1605.
148. Gropler, R.J.; Geltman, E.M.; Sampathkumaran, K.; Perez, J.E.; Schechtman, K.B.; Conversano, A.; Sobel, B.E.; Bergmann, S.R.; Siegel, B.A. Comparison of Carbon-11-Acetate with Fluorine-18 Fluorodeoxyglucose for Delineating Viable Myocardium by Positron Emission Tomography. J. Am. Coll. Cardiol. **1993**, *22*, 1587–1597.
149. Wolpers, H.G.; Burchert, W.; van den Hoff, J.; Weinhardt, R.; Meyer, G.J.; Lichtlen, P.R. Assessment of Myocardial Viability by Use of ^{11}C-Acetate and Positron Emission Tomography: Threshold Criteria of Reversible Dysfunction. Circulation **1997**, *95*, 1417–1424.
150. Hasegawa, S.; Uehara, T.; Yamaguchi, H.; Fujino, K.; Kusuoka, H.; Hori, M.; Nishimura, T. Validity of ^{18}F-Fluorodeoxyglucose Imaging with a Dual-Head Coincidence Gamma Camera for Detection of Myocardial Viability. J. Nucl. Med. **1999**, *40*, 1884–1892.
151. Bax, J.J.; Wijns, W. Fluorodeoxyglucose Imaging to Assess Myocardial Viability: PET, SPECT or Gamma Camera Coincidence Imaging? J. Nucl. Med. **1999**, *40*, 1893–1895.
152. De Sutter, J.; De Winter, F.; Van de Wiele, C.; De Bondt, P.; D'Asseler, Y.; Dierckx, R. Cardiac Fluorine-18 Fluorodeoxyglucose Imaging Using a Dual-Head Gamma Camera with Coincidence Detection: A Clinical Pilot Study. Eur. J. Nucl. Med. **2000**, *27*, 676–685.
153. von Kienlin, M.; Beer, M.; Greiser, A.; Hahn, D.; Harre, K.; Köstler, H.; Landshütz, W.; Pabst, T.; Sandstede, J.; Neubauer, S. Advances in Human Cardiac ^{31}P-MR Spectroscopy: SLOOP and Clinical Applications. J. Magn. Reson. Imaging. **2001**, *13*, 521–527.
154. Kalil-Filho, R.; de Albuquerque, C.P.; Weiss, R.G.; Mocelim, A.; Bellotti, G.; Cerri, G.; Pileggi, F. Normal High Energy Phosphate Ratios in "Stunned" Human Myocardium. J. Am. Coll. Cardiol. **1997**, *30*, 1228–1232.
155. Yabe, T.; Mitsunami, K.; Inubushi, T.; Kinoshita, M. Quantitative Measurements of Cardiac Phosphorus

Metabolites in Coronary Artery Disease by Phosphorus-31 Magnetic Resonance Spectroscopy. Circulation **1995**, *92*, 15–23.
156. Beer, M.; Hahn, D.; Neubauer, S. Human Cardiac MR Spectroscopy—Clinical Methods and Applications. MAGMA **1998**, *6*, 113–115.
157. Yabe, T.; Mitsunami, K.; Okada, K.; Morikawa, S.; Inubushi, T.; Kinoshita, M. Detection of Myocardial Ischemia by ^{31}P Magnetic Resonance Spectroscopy During Handgrip Exercise. Circulation **1994**, *89*, 1709–1716.
158. Pohost, G.M. Is ^{31}P-NMR Spectroscopic Imaging a Viable Approach to Assess Myocardial Viability? Circulation **1995**, *92*, 9–10.
159. Buchthal, S.D.; den Hollander, J.A.; Merz, N.; Rogers, W.J.; Pepine, C.J.; Reichek, N.; Sharaf, B.L.; Reis, S.; Kelsey, S.F.; Pohost, G.M. Abnormal Myocardial Phosphorus-31 Nuclear Magnetic Resonance Spectroscopy in Women with Chest Pain but Normal Coronary Angiograms. N. Engl. J. Med. **2000**, *342*, 829–835.
160. Butterworth, E.J.; Evanochko, W.T.; Pohost, G.M. The 31 P-NMR Stress Test: An Approach for Detecting Myocardial Ischemia. Ann. Biomed. Eng. **2000**, *28*, 930–933.
161. Hetherington, H.P.; Luney, D.J.E.; Vaughan, J.T.; Pan, J.W.; Ponder, S.L.; Tschendel, O.; Twieg, D.B.; Pohost, G.M. 3-D ^{31}P Spectroscopic Imaging of the Human Heart at 4.1 T. Magn. Reson. Med. **1995**, *33*, 427–431.
162. Pettigrew, R.I.; Oshinski, J.N.; Chatzimavroudis, G.; Dixon, W.T. MRI Techniques for Cardiovascular Imaging. J. Magn. Reson. Imaging. **1999**, *10*, 590–601.
163. Pflugfelder, P.W.; Wisenberg, G.; Prato, F.S.; Carroll, S.E.; Turner, K.L. Early Detection of Canine Myocardial Infarction by Magnetic Resonance Imaging In Vivo. Circulation **1985**, *71* (3), 587–594.
164. Bouchard, A.; Reeves, R.C.; Cranney, G.; Bishop, S.P.; Pohost, G.M. Assessment of Myocardial Infarct Size by Means of T_2-weighted 1H Nuclear Magnetic Resonance Imaging. Am. Heart. J. **1989**, *117*, 281–289.
165. Ryan, T.; Tarver, R.D.; Duerk, J.L.; Sawada, S.G.; Hollenkamp, N.C.; Johnson, J.; Hobson, A.; Sims, J. Distinguishing Viable from Infarcted Myocardium After Experimental Ischemia and Reperfusion by Using Nuclear Magnetic Resonance Imaging. J. Am. Coll. Cardiol. **1990**, *15*, 1355–1364.
166. Higgins, C.B.; Herfkens, R.; Lipton, M.J.; Sievers, R.; Sheldon, P.; Kaufman, L.; Crooks, L.E. Nuclear Magnetic Resonance Imaging of Acute Myocardial Infarction in Dogs: Alterations in Magnetic Relaxation Times. Am. J. Cardiol. **1983**, *52*, 184–188.
167. Wesbey, G.E.; Higgins, C.B.; Lanzer, P.; Botvinick, E.; Lipton, M.J. Imaging and Characterization of Acute Myocardial Infarction by Gated Nuclear Magnetic Resonance. Circulation **1984**, *69*, 125–130.
168. Ratner, A.V.; Okada, R.D.; Goldman, M.R.; O'Keefe, D.D.; Newell, J.B.; Pohost, G.M. Early Detection of Myocardial Ischemic Damage Using Proton NMR Techniques. Circulation **1983**, *68* (Suppl. III), III-387.
169. Johnston, D.L.; Brady, T.J.; Ratner, A.V.; Rosen, B.R.; Newell, J.B.; Pohost, G.M.; Okada, R.D. Assessment of Myocardial Ischemia with Proton Magnetic Resonance Effects on a Three Hour Coronary Occlusion with and Without Reperfusion. Circulation **1985**, *71*, 595–601.
170. Garcia-Dorado, D.; Oliveras, J.; Gili, J.; Sanz, E.; Perez-Villa, F.; Barrabes, J.; Carreras, M.J.; Solares, J.; Soler-Soler, J. Analysis of Myocardial Oedema by Magnetic Resonance Imaging Early After Coronary Artery Occlusion with or without Reperfusion. Cardiovasc. Res. **1993**, *27*, 1462–1469.
171. McNamara, M.T.; Higgins, C.B.; Schechtmann, N.; Botinivick, E.; Amparo, E.G.; Chatterjee, K. Detection and Characterization of Acute Myocardial Infarctions in Man Using Gated Magnetic Resonance Imaging. Circulation **1985**, *71*, 717–724.
172. Pohost, G.M.; Goldman, N.R.; Pykett, I.L.; Brady, T.J.; Foak, R.A.; Buanno, F.S.; Dinsmore, R.E.; Miller, S.W.; Weyman, A.E.; Kistler, J.P.; Hinshaw, W.S. Gated NMR Imaging in Canine Myocardial Infarction. Circulation **1982**, *66* (Suppl. II), II-30.
173. McNamara, M.T.; Tscholakoff, D.; Revel, D.; Soulen, R.; Schechtmann, H.; Botvinick, E. Differentiation of Reversible and Irreversible Myocardial Injury by MR Imaging with and without Gd-DTPA. Radiology **1986**, *158*, 765–769.
174. Lim, T.-H.; Hong, M.K.; Lee, J.S.; Mun, C.W.; Park, S.J.; Ryu, J.S.; Lee, J.H.; Chien, D.; Laub, G. Novel Application of Breath-Hold Turbo Spin–Echo T_2 MRI for Detection of Acute Myocardial Infarction. J. Magn. Reson. Imaging. **1997**, *7*, 996–1001.
175. Choi, S.I.; Jiang, C.Z.; Lim, K.H.; Kim, S.T.; Lim, C.H.; Gong, G.Y.; Lim, T-H. Application of Breath-Hold T_2-Weighted First-Pass Perfusion and Gadolinium-Enhanced T_1-weighted MR Imaging for Assessment of Myocardial Viability in a Pig Model. J. Magn. Reson. Imaging. **2000**, *11*, 476–480.
176. VanRugge, F.P.; van der Wall, E.E.; Spanjersberg, S.J.; deRoos, A.; Matheijssen, N.A.A.; Zwinderman, A.H.; van Dijkman, P.R.M.; Reiber, J.H.C.; Bruschke, A.V.G. Magnetic Resonance Imaging During Dobutamine Stress for Detection and Localization of Coronary Artery Disease: Quantitative Wall Motion Analysis Using a Modification of the Centerline Method. Circulation **1994**, *90*, 127–138.
177. Baer, F.M.; Thiessen, P.; Scheider, C.A.; Voth, E.; Sechtem, U.; Schicha, H.; Erdmann, E. Dobutamine Magnetic Resonance Imaging Predicts Contractile Recovery of Chronically Dysfunctional Myocardium After Successful Revascularization. J. Am. Coll. Cardiol. **1998**, *31*, 1040–1048.

178. Oshinski, J.N.; Han, H.-C.; Ku, D.N.; Pettigrew, R.I. Quantitative Prediction of Improvement in Cardiac Function After Revascularization with MR Imaging and Modeling: Initial Results. Radiology **2001**, *221*, 515–521.
179. Nagel, E.; Lehmkuhl, H.B.; Bocksch, W.; Klein, C.; Vogel, U.; Frantz, E.; Ellmer, A.; Dreysse, S.; Fleck, E. Noninvasive Diagnosis of Ischemia Induced Wall Motion Abnormalities with the Use of High-Dose Dobutamine Stress-MRI. Circulation **1999**, *99*, 763–770.
180. Axel, L.; Dougherty, L. Heart Wall Motion: Improved Method of Spatial Modulation of Magnetization for MR Imaging. Radiology **1989**, *172*, 349–350.
181. Zerhouni, E.A.; Parish, D.M.; Rogers, W.J.; Yang, A.; Shapiro, E.P. Human Heart: Tagging with MR Imaging—A Method for Noninvasive Assessment of Myocardial Motion. Radiology **1988**, *169*, 59–63.
182. Kraitchman, D.L.; Hillenbrand, H.B.; Oznur, I.; Lima, J.A.C.; McVeigh, E.R.; Zerhouni, E.A.; Bluemke, D.A. Noninvasive Assessment of Myocardial Stunning From Short-Term Coronary Occlusion Using Tagged Magnetic Resonance Imaging. J. Cardiovasc. Magn. Reson. **2000**, *2* (2), 123–136.
183. Weinmann, H.J.; Laniado, M.; Mutzel, W. Pharmacokinetics of Gd-DTPA/Dimeglumine After Intravenous Injection into Healthy Volunteers. Physiol. Chem. Phys. Med. NMR **1984**, *16*, 167–172.
184. Prato, F.S.; Wisenberg, G.; Marshall, T.P.; Uksik, P.; Zabel, P. Comparison of the Biodistribution of Gadolinium-153 DTPA and Technetium-99m DTPA in Rats. J. Nucl. Med. **1988**, *29* (10), 1683–1687.
185. de Roos, A.; Matheijssen, N.A.; Doornbos, J.; van Dijkman, P.R.; van Voorthuisen, A.E.; van der Wall, E.E. Myocardial Infarct Size After Reperfusion Therapy: Assessment with Gd-DTPA-Enhanced MR Imaging. Radiology **1990**, *176*, 517–521.
186. Diesbourg, L.D.; Prato, F.S.; Wisenberg, G.; Drost, D.J.; Marshall, T.P.; Carroll, S.E.; O'Neill, B. Quantification of Myocardial Blood Flow and Extracellular Volumes Using a Bolus Injection of Gd-DTPA: Kinetic Modeling in Canine Ischemic Heart Disease. Magn. Reson. Med. **1992**, *23*, 239–253.
187. Kim, R.J.; Chen, E.; Lima, J.A.C.; Judd, R.M. Myocardial Gd-DTPA Kinetics Determine MRI Contrast Enhancement and Reflect the Extent and Severity of Myocardial Injury Following Acute Reperfused Infarction. Circulation **1996**, *94*, 3318–3326.
188. Wilke, N.; Jerosch-Herold, M. Assessing Myocardial Perfusion in Coronary Artery Disease with Magnetic Resonance First-Pass Imaging. Cardiol. Clin. **1998**, *16*, 227–246.
189. Jerosch-Herold, M.; Wilke, N.; Stillman, A.E.; Wilson, R.F. Magnetic Resonance Quantification of the Myocardial Perfusion Reserve with a Fermi Function Model for Constrained Deconvolution. Med. Phys. **1998**, *25*, 73–84.
190. Edelman, R.; Li, W. Contrast-Enhanced Echo-Planar MR Imaging of Myocardial Perfusion: Preliminary Study in Humans. Radiology **1994**, *190*, 771–777.
191. Manning, W.; Atkinson, D.; Grossman, W.; Paulin, S.; Edelman, R.R. First-Pass Nuclear Magnetic Resonance Imaging Studies Using Gadolinium-DTPA in Patients with Coronary Artery Disease. J. Am. Coll. Cardiol. **1991**, *18*, 959–965.
192. Wilke, N.; Jerosch-Herold, M.; Wang, Y.; Huang, Y.; Christensen, B.V.; Stillman, A.E.; Ugurbil, K.; McDonald, K.; Wilson, R.F. Myocardial Perfusion Reserve: Assessment with Multisection, Quantitative, First-Pass MR Imaging. Radiology **1997**, *204*, 373–384.
193. Bertschinger, K.M.; Nanz, D.; Buechi, M.; Luescher, T.F.; Marincek, B.; von Schulthess, G.K.; Schwitter, J. Magnetic Resonance Myocardial First-Pass Perfusion Imaging: Parameter Optimization for Signal Response and Cardiac Coverage. J. Magn. Reson. Imaging. **2001**, *14*, 556–562.
194. Wilson, R.F.; Laughlin, D.E.; Ackell, P.H.; Chilian, W.M.; Holida, M.D.; Hartley, C.J.; Armstrong, M.L.; Marcus, M.L.; White, C.W. Transluminal, Subselective Measurement of Coronary Artery Blood Flow Velocity and Vasodilator Reserve in Man. Circulation **1985**, *72*, 82–92.
195. Ito, B.R.; Libraty, D.H.; Engler, R.L. Effect of Transient Coronary Occlusion on Coronary Blood Flow Autoregulation, Vasodilator Reserve and Response to Adenosine in the Dog. J. Am. Coll. Cardiol. **1991**, *18*, 858–867.
196. Klocke, F.J.; Simonetti, O.P.; Judd, R.M.; Kim, R.J.; Harris, K.R.; Hedjbeli, S.; Fieno, D.S.; Miller, S.; Chen, V.; Parker, M.A. Limits of Detection of Regional Differences in Vasodilated Flow in Viable Myocardium by First-Pass Magnetic Resonance Perfusion Imaging. Circulation **2001**, *104*, 2412–2416.
197. Keijer, J.T.; van Rossum, A.C.; van Eenige, M.J.; Bax, J.J.; Visser, F.C.; Teule, J.J.; Visser, C.A. Magnetic Resonance Imaging of Regional Myocardial Perfusion in Patients with Single-Vessel Coronary Artery Disease: Quantitative Comparison with 201Thallium-SPECT and Coronary Angiography. J. Magn. Reson. Imaging. **2000**, *11*, 607–615.
198. Canet, E.P.; Janier, M.F.; Revel, D. Magnetic Resonance Perfusion Imaging in Ischemic Heart Disease. J. Magn. Reson. Imaging. **1999**, *10*, 423–433.
199. Arheden, H.; Saeed, M.; Higgins, C.B.; Gao, D.W.; Bremerich, J.; Wyttenbach, R.; Dae, M.W.; Wendland, M.F. Measurement of the Distribution Volume of Gadopentetate Dimeglumine at Echo-Planar MR Imaging to Quantify Myocardial Infarction: Comparison with ^{99m}Tc-DTPA Autoradiography in Rats. Radiology **1999**, *211*, 698–708.

200. Arheden, H.; Saeed, M.; Higgins, C.B.; Gao, D.-W.; Ursell, P.C.; Bremerich, J.; Wyttenbach, R.; Dae, M.W.; Wendland, M.F. Reperfused Rat Myocardium Subjected to Various Durations of Ischemia: Estimation of the Distribution Volume of Contrast Material with Echo-Planar MR Imaging. Radiology **2000**, *215*, 520–528.
201. Wendland, M.F.; Saeed, M.; Lauerma, K.; Derugin, N.; Mintorovitch, J.; Cavagna, F.M.; Higgins, C.B. Alterations in T_1 of Normal and Reperfused Infarcted Myocardium After Gd-BOPTA Versus Gd-DTPA on Inversion Recovery EPI. Magn. Reson. Med. **1997**, *37*, 448–456.
202. Saeed, M.; Lund, G.; Wendland, M.F.; Bremerich, J.; Weinmann, H.; Higgins, C.B. Magnetic Resonance Characterization of the Peri-infarction Zone of Reperfused Myocardial Infarction with Necrosis-specific and Extracellular Contrast Media. Circulation **2001**, *103*, 871–876.
203. Oshinski, J.N.; Yang, Z.; Jones, J.R.; Mata, J.F.; French, B.A. Imaging Time After Gd-DTPA Injection is Critical in Using Delayed Enhancement to Determine Infarct Size Accurately with Magnetic Resonance Imaging. Circulation **2001**, *104*, 2838–2842.
204. Inoue, S.-I.; Murakami, Y.; Ochiai, K.; Kitamura, J.; Ishibashi, Y.; Kawamitsu, H.; Sugimura, K.; Shimada, T. The Contributory Role of Interstitial Water in Gd-DTPA-enhanced MRI in Myocardial Infarction. J. Magn. Reson. Imaging. **1999**, *9*, 215–219.
205. Judd, R.M.; Lugo-Olivieri, C.H.; Arai, M.; Kondo, T.; Croisille, P.; Lima, J.A.C.; Mohan, V.; Becker, L.C.; Zerhouni, E.A. Physiological Basis of Myocardial Contrast Enhancement in Fast Magnetic Resonance Images of 2-Day-Old Reperfused Canine Infarcts. Circulation **1995**, *92*, 1902–1910.
206. Wu, K.C.; Kim, R.J.; Bluemke, D.A.; Rochitte, C.E.; Zerhouni, E.A.; Becker, L.C.; Lima, J.A.C. Quantification and Time Course of Microvascular Obstruction by Contrast-Enhanced Echocardiography and Magnetic Resonance Imaging Following Acute Myocardial Infarction and Reperfusion. J. Am. Coll. Cardiol. **1998**, *32*, 1756–1764.
207. Gerber, B.L.; Rochitte, C.E.; Bluemke, D.A.; Melin, J.A.; Croisille, P.; Becker, L.C.; Lima, J.A.C. Relation Between Gd-DTPA Contrast Enhancement and Regional Inotropic Response in the Periphery and Center of Myocardial Infarction. Circulation **2001**, *104*, 998–1004.
208. Hillenbrand, H.B.; Kim, R.J.; Parker, M.A.; Fieno, D.S.; Judd, R.M. Early Assessment of Myocardial Salvage by Contrast-Enhanced Magnetic Resonance Imaging. Circulation **2000**, *102*, 1678–1683.
209. Fieno, D.S.; Kim, R.J.; Chen, E.-L.; Lomasney, J.W.; Klocke, F.J.; Judd, R.M. Contrast-Enhanced Magnetic Resonance Imaging of Myocardium at Risk: Distinction Between Reversible and Irreversible Injury Throughout Infarct Healing. J. Am. Coll. Cardiol. **2000**, *36*, 1985–1991.
210. Rogers, W.J.; Kramer, C.M.; Geskin, G.; Hu, Y.-L.; Theobald, T.M.; Vido, D.A.; Petruolo, S.; Reichek, N. Early Contrast-Enhanced MRI Predicts Late Functional Recovery After Reperfused Myocardial Infarction. Circulation **1999**, *99*, 744–750.
211. Dendale, P.; Franken, P.R.; Block, P.; Pratikakis, Y.; de Roos, A. Contrast Enhanced and Functional Magnetic Resonance Imaging for the Detection of Viable Myocardium After Infarction. Am. Heart. J. **1998**, *135*, 875–880.
212. Choi, K.M.; Kim, R.J.; Gubernikoff, G.; Vargas, J.D.; Parker, M.; Judd, R.M. Transmural Extent of Acute Myocardial Infarction Predicts Long-Term Improvement in Contractile Function. Circulation **2001**, *104*, 1101–1107.
213. Sandstede, J.J.W.; Beer, M.; Lipke, C.C.; Pabst, T.; Kenn, W.; Harre, K.; Neubauer, S.; Hahn, D. Time Course of Contrast Enhancement Patterns After Gd-BOPTA in Correlation to Myocardial Infarction and Viability: A Feasibility Study. J. Magn. Reson. Imaging. **2001**, *14*, 789–794.
214. Ramani, K.; Judd, R.M.; Holly, T.A.; Parrish, T.B.; Rigolin, V.H.; Parker, M.A.; Callahan, C.; Fitzgerald, S.W.; Bonow, R.O.; Klocke, F.J. Contrast Magnetic Resonance Imaging in the Assessment of Myocardial Viability in Patients with Stable Coronary Artery Disease and Left Ventricular Dysfunction. Circulation **1998**, *98*, 2687–2694.
215. Sandstede, J.J.W.; Lipke, C.; Beer, M.; Harre, L.; Pabst, T.; Kenn, W.; Neubauer, S.; Hahn, D. Analysis of First-Pass and Delayed Contrast-Enhancement Patterns of Dysfunctional Myocardium on MR Imaging: Use in the Prediction of Myocardial Viability. Am. J. Roentgenol. **2000**, *174*, 1737–1740.
216. Kim, R.J.; Wu, E.; Rafael, A.; Chen, E.-L.; Parker, M.A.; Simonetti, O.; Klocke, F.J.; Bonow, R.O.; Judd, R.M. The Use of Contrast-Enhanced Magnetic Resonance Imaging to Identify Reversible Myocardial Dysfunction. N. Engl. J. Med. **2000**, *343*, 1445–1453.
217. Wu, E.; Judd, R.M.; Vargas, J.D.; Klocke, F.J.; Bonow, R.O.; Kim, R.J. Visualisation of Presence, Location, and Transmural Extent of Healed Q-Wave and Non-Q-Wave Myocardial Infarction. Lancet **2001**, *357*, 21–28.
218. Lauerma, K.; Niemi, P.; Hanninen, H.; Janatuinen, T.; Voipio-Pulkki, L.-M.; Knuuti, J.; Toivonen, L.; Makela, T.; Makijarvi, M.A.; Aronen, H.J. Multimodality MR Imaging Assessment of Myocardial Viability: Combination of First-Pass and Late Contrast Enhancement to Wall Motion Dynamics and Comparison with FDG PET—Initial Experience. Radiology **2000**, *217*, 729–736.

219. Klein, C.; Nekolla, S.G.; Bengel, F.M.; Momose, M.; Sammer, A.; Haas, F.; Schnackenburg, B.; Delius, W.; Mudra, H.; Wolfram, D.; Schwaiger, M. Assessment of Myocardial Viability with Contrast-Enhanced Magnetic Resonance Imaging: Comparison with Positron Emission Tomography. Circulation **2002**, *105*, 162–167.
220. de Roos, A.; Doornbos, J.; van der Wall, E.E.; van Voorthuisen, A.E. MR Imaging of Acute Myocardial Infarction: Value of Gd-DTPA. Am. J. Roentgenol. **1988**, *150*, 531–534.
221. Ricciardi, M.J.; Wu, E.; Davidson, C.J.; Choi, K.M.; Klocke, F.J.; Bonow, R.O.; Judd, R.M.; Kim, R.J. Visualization of Discrete Microinfarction After Percutaneous Coronary Intervention Associated with Mild Creatine Kinase-MB Elevation. Circulation **2001**, *103*, 2780–2783.
222. Tong, C.Y.; Prato, F.S.; Wisenberg, G.; Lee, T-Y.; Carroll, E.; Sandler, D.; Wills, J. Techniques for the Measurement of the Local Myocardial Extraction Efficiency for Inert Diffusible Contrast Agents Such as Gadopentate Dimeglumine. Magn. Reson. Med. **1993**, *30*, 332–336.
223. Bellamy, D.D.; Pereira, R.S.; McKenzie, C.A.; Prato, F.S.; Drost, D.J.; Sykes, J.; Wisenberg, G. Gd-DTPA Bolus Tracking in the Myocardium Using T_1 Fast Acquisition Relaxation Mapping (T_1 FARM). Magn. Reson. Med. **2001**, *46*, 555–564.
224. Pereira, R.S.; Prato, F.S.; Wisenberg, G.; Sykes, J. The Determination of Myocardial Viability Using Gd-DTPA in a Canine Model of Acute Myocardial Ischemia and Reperfusion. Magn. Reson. Med. **1996**, *36*, 684–693.
225. Pereira, R.S.; Prato, F.S.; Sykes, J.; Wisenberg, G. Assessment of Myocardial Viability Using MRI During a Constant Infusion of Gd-DTPA: Further Studies at Early and Late Periods of Reperfusion. Magn. Reson. Med. **1999**, *42*, 60–68.
226. Pereira, R.S.; Prato, F.S.; Lekx, K.S.; Sykes, J.; Wisenberg, G. Contrast-Enhanced MRI for the Assessment of Myocardial Viability After Permanent Coronary Artery Occlusion. Magn. Reson. Med. **2000**, *44*, 309–316.
227. Pereira, R.S.; Prato, F.S.; Wisenberg, G.; Yvorchuk, K. Clinical Assessment of Myocardial Viability Using MRI During a Constant Infusion of Gd-DTPA. MAGMA **2000**, *11*, 104–113.
228. Flacke, S.J.; Fischer, S.E.; Lorenz, C.H. Measurement of the Gadopentetate Dimeglumine Partition Coefficient in Human Myocardium In Vivo: Normal Distribution and Elevation in Acute and Chronic Infarction. Radiology **2001**, *218*, 703–710.
229. Thornhill, R.E.; Prato, F.S.; Pereira, R.S.; Wisenberg, G.; Sykes, J. Examining a Canine Model of Stunned Myocardium with Gd-DTPA-Enhanced MRI. Magn. Reson. Med. **2001**, *45*, 864–871.
230. Lekx, K.S.; Prato, F.S.; Sykes, J.; Wisenberg, G. A Canine Model of Hibernating Myocardium Using Magnetic Resonance Imaging with Gd-DTPA. In Proceedings of the International Society for Magnetic Resonance in Medicine, ISMRM-ESMRMB Joint Annual Meeting, Glasgow, Scotland, UK, April 21–27, 2001; 1908.
231. Flamm, S.D.; Villareal, R.P.; Hariharan, R.; Muthupillai, R.; Massumi, A.G.; Wilson, J.M. Delayed-Enhancement MRI Reveals Myocardial Fibrosis in Patients with Symptomatic Hypertrophic Cardiomyopathy. In Proceedings of the International Society for Magnetic Resonance in Medicine, ISMRM-ESMRMB Joint Annual Meeting, Glasgow, Scotland, UK, April 21–27, 2001; 226.
232. Wassmuth, R.; Aletras, A.H.; Begley, D.A.; Bove Bettis, K.E.; Agyeman, K.O.; Fananapazir, L.; Arai, A.E. Delayed hyperenhancement detects myocardial abnormalities. In Proceedings of the International Society for Magnetic Resonance in Medicine, ISMRM-ESMRMB Joint Annual Meeting, Glasgow, Scotland, UK, April 21–27, 2001; 227.
233. Sipola, P.; Lauerma, K.; Kuikka, J.T.; Vanninen, E.; Peuhkurinen, K.; Jaaskelainen, P.; Laasko, M.; Manninen, H.; Kuusisto, J.; Aronen, H.J. Assessment of Myocardial Fibrosis in Hypertrophic Cardiomyopathy with First Pass and Delayed T1 Enhancement. In Proceedings of the International Society for Magnetic Resonance in Medicine, ISMRM-ESMRMB Joint Annual Meeting, Glasgow, Scotland, UK, April 21–27, 2001; 228.
234. Cannon, P.J.; Maudsley, A.A.; Hilal, S.K.; Simon, H.E.; Cassidy, F. Sodium Nuclear Magnetic Resonance Imaging of Myocardial Tissue of Dogs After Coronary Artery Occlusion and Reperfusion. J. Am. Coll. Cardiol. **1987**, *7*, 573–579.
235. Kim, R.J.; Lima, J.A.C.; Chen, E.-L.; Reeder, S.B.; Klocke, F.J.; Zerhouni, E.A.; Judd, R.M. Fast ^{23}Na Magnetic Resonance Imaging of Acute Reperfused Myocardial Infarction: Potential to Assess Myocardial Viability. Circulation **1997**, *95*, 1877–1885.
236. Kim, R.J.; Judd, R.M.; Chen, E.-L.; Fieno, D.S.; Parrish, T.B.; Lima, J.A.C. Relationship of Elevated ^{23}Na Magnetic Resonance Image Intensity to Infarct Size After Acute Reperfused Myocardial Infarction. Circulation **1999**, *100*, 185–192.
237. Kupriyanov, V.V.; Xiang, B.; Sun, J.; Dai, G.; Jilkina, O.; Dao, V.; Deslauriers, R. Three-Dimensional ^{87}Rb NMR Imaging and Spectroscopy of K^+ Fluxes in Normal and Postischemic Pig Hearts. Magn. Reson. Med. **2000**, *44*, 83–91.
238. Kupriyanov, V.V.; Dai, G.; Shaw, R.A.; Sun, J.; Jilkina, O.; Luo, Z.; Mantsch, H.; Deslauriers, R. Noninvasive Assessment of Cardiac Ischemic Injury Using ^{87}Rb and

^{23}Na Imaging, ^{31}P MR and Optical Spectroscopy. Magn. Reson. Med. **2000**, *44*, 899–908.

239. Pagano, D.; Bonser, R.S.; Townend, J.N.; Ordoubadi, F.; Lorenzoni, R.; Camici, P.G. Predictive Value of Dobutamine Echocardiography and Positron Emission Tomography in Identifying Hibernating Myocardium in Patients with Postischaemic Heart Failure. Heart **1998**, *79*, 281–288.
240. Jadvar, H.; Strauss, H.W.; Segall, G.M. SPECT and PET in the Evaluation of Coronary Artery Disease. Radiographics **1999**, *19*, 915–926.
241. Naylor, C.D.; Slaughter, P.M. *Cardiovascular Health and Services in Ontario-An ICES Atlas*; Institute for Clinical Evaluative Sciences, Contintental Press, Toronto, Canada 1999.

Received May 31, 2001
Accepted March 12, 2002